★★ DRAFT ★★

SECTION 8.2.1.2.3

CASTOR X TSAR

General Nuclear Systems, Inc.
Columbia, SC
December, 1992

9212300283 921228
PDR PROJ
M-50 CF

ANALYSIS OF FUEL BASKETS

The two options of the fuel baskets (X/28 and X/33) are analyzed in this section to show that the stress in the baskets during the accident conditions are within the allowable values. The CASTOR X casks are required to use an impact limiter if they are stored at a storage pad which has not been designed as a Seismic Class I Structure, in which case the cask may have a potential for an accidental tip-over. It has been established in Section 8.2.1.2.3.1 that the maximum deceleration during the tip-over accident will be 24 g's for X/28 casks and 8.2 g's for the X/33 casks. The fuel basket are assumed to undergo the same lateral deceleration.

The stress limits for the accident condition loads are based upon the design criteria of Table 3.2-1. The limiting stress values are calculated in accordance with the ASME Code /Ref. 8.2-15/, Appendix F and Reg. Guide 7.6.

CASTOR X/28 BASKET

A detailed finite element analysis of the CASTOR X/28 fuel basket was performed using the ANSYS general purpose finite element computer program. An impact limiter is used on the cask during the storage at the pad, as described in section 8.2.1.2.3.1 of the TSAR. The peak deceleration at the worst location in the cask is 24 g's. This acceleration occurs at the top end of the cask, but is conservatively assumed to be applied uniformly at all points along the axis of the cask. The fuel basket geometry is shown in Figure 8.2-14.

The CASTOR X/28 basket is constructed in five separate components. The inner basket is comprised of four quarter sections which are inserted into the outer basket assembly. The quarter sections are identical in design and chevron shaped spacers are used to position in the inner assemblies. The inner basket is supported radially and tangentially by the outer basket assembly. Shear blocks at 0°, 90°, 180°, and 270° provide tangential support for a horizontal acceleration load. The basket is supported on the inner ring of the outer basket assembly for radial loadings.

Because the basket is built in separate components, it is convenient to analyze the inner and outer baskets separately. The inner basket model is supported radially and tangentially as previously discussed for both the 90°-270° drop orientation (hereinafter referred to as the "vertical" direction) and the 45°-225° drop orientation (hereinafter referred to as the 45° orientation). Another intermediate orientation at 67½° was also analyzed. The vertical drop can be evaluated using a 180° model. The 45° and 67½° drop were evaluated using a full 360° model.

The inner basket analysis was conducted by applying a uniform acceleration to the model to simulate the peak g loading. The correct material densities were used for all components. The fuel elements were simulated by applying a pressure load to the "bottom" of the fuel slots to produce an equivalent g load on the basket. Due to the repeating pattern of spacer plates along the longitudinal axis of the cask, the basket was modeled by considering only a 19.68 inch (500mm) long piece of the basket. Symmetry planes at each end were maintained

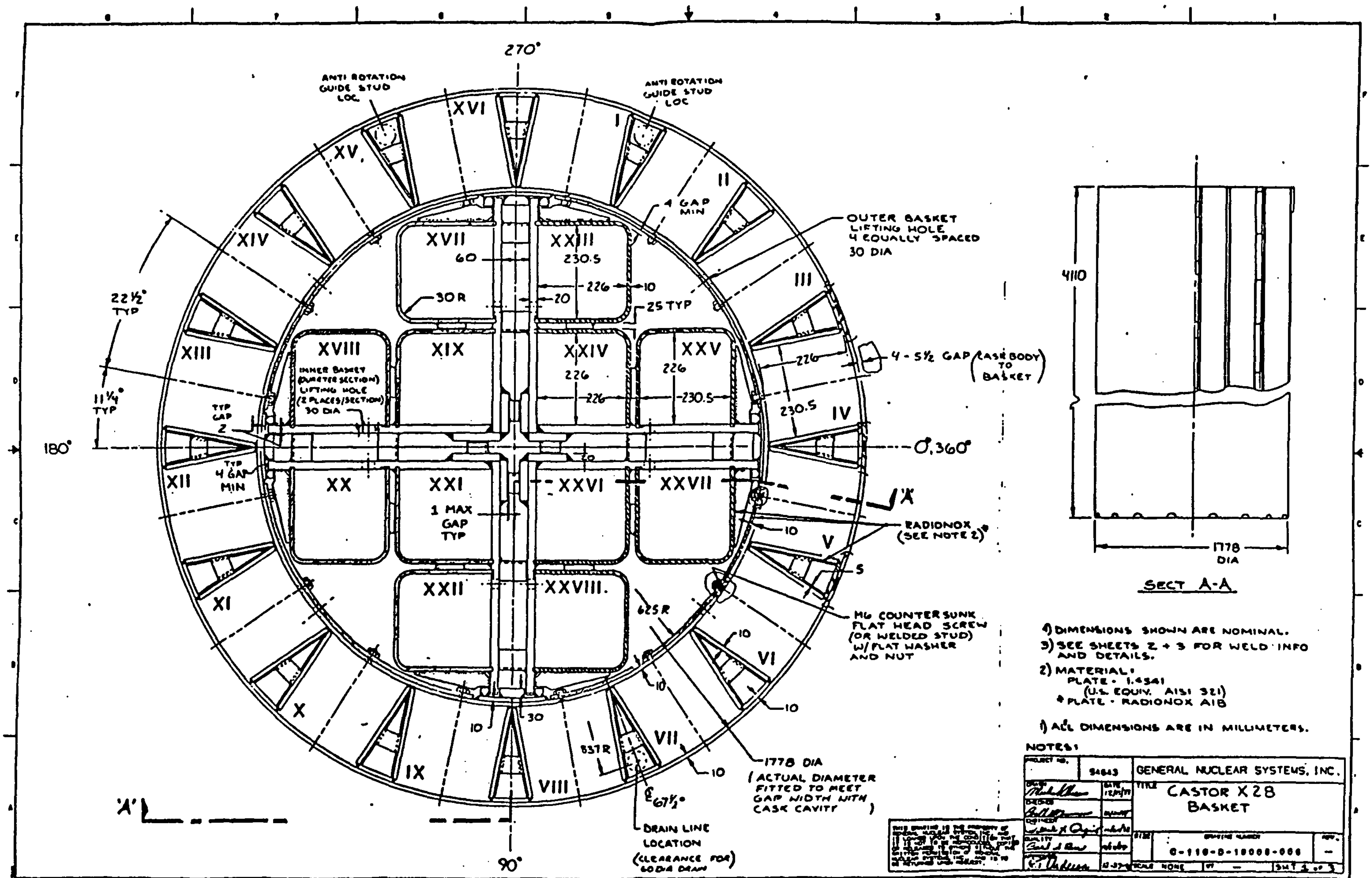

<u>Figure 8.2-14</u>
<u>CASTOR X/28 Basket Geometry</u>

by coupling the nodes at the cut plane. A detailed discussion of the boundary conditions used in the fuel basket analyses is presented in the GNSI proprietary document ST-128 /Ref. 8.2-21/.

The reaction loads obtained from the analysis of the inner basket were used in evaluating the outer basket. The radial and tangential loads calculated for the side drop were applied to the outer basket models as nodal forces. Radial restraint was applied to the outer basket to simulate the cask inner wall. Reaction forces due to tip-over of the cask in various basket orientations are listed in Table 8.2-3. Figures 8.2-15 through 8.2-17 show the positive direction of the reaction forces at various locations of the inner basket. The opposite forces as shown in these figures were applied to the outer basket in the corresponding orientation.

The resulting stress distributions for the inner basket for the vertical direction are provided in Figures 8.2-18 through 8.2-20. Figures 8.2-21 through 8.2-24 present the stress distribution in the outer basket. Figures 8.2-25 through 8.2-41 show the stress distribution for 45° and 67½° orientations. The figures are clearly labeled to identify the orientations and the basket components to which they apply. Please note that the stress contours shown on the figures are in-plane stresses, not the stress intensities. These figures are also referred to in the buckling evaluation of the plates presented in the subsequent section of this TSAR.

Table 8.2-4 provides a summary of the maximum stress intensities in various components of the fuel basket due to accidental tip-over in different orientations of the basket. The actual temperature of different components of the basket may be determined from Section 5.1.3, Figure 5.1-11 of the TSAR. The outer basket temperature is approximately 260°C (25.7 Kw). The allowable stress for the inner basket is, therefore, based on 260°C temperature. The inner basket is somewhat hotter and the allowable stress is based upon 350°C.

It can be seen from Table 8.2-4, the stresses are well below the limits in all cases. The highest stress occurs in the small gusset plate which supports the basket. The stress is very local and failure of this component would not lead to failure of the basket, only a redistribution of stress in the component will take place.

Table 8.2-3
Reaction Forces at the Inner Basket
of CASTOR X/28 Cask
Due to Tip-Over Accident
in Various Basket Orientations

Location[1]	Reaction Force[2], lbs					
	0°-Orientation		45°-Orientation		67½°-Orientation	
	Radial	Tangential	Radial	Tangential	Radial	Tangential
A	N/A[3]	N/A	33,272	12,912	43,792	13,288
B	47,480	7,692	33,592	2,837	43,816	7,842
C	5,024	6,212	33,552	2,834	18,152	2,614
D	0	8,096	33,600	12,960	18,152	10,632
E	N/A	3,184	0	9,504	0	8,264
F	N/A	N/A	0	757	0	2,691
G	N/A	N/A	0	741	0	4,073
H	N/A	N/A	0	9,496	0	9,296

NOTES:

(1) Please refer to Figures 8.2-15 through 8.2-17 for locations of indicated points. The positive direction of the reactions is as indicated in these figures.

(2) The reaction forces correspond to 19.68 inch (500mm) axial length of the basket.

(3) Not available because only 180° model was analyzed.

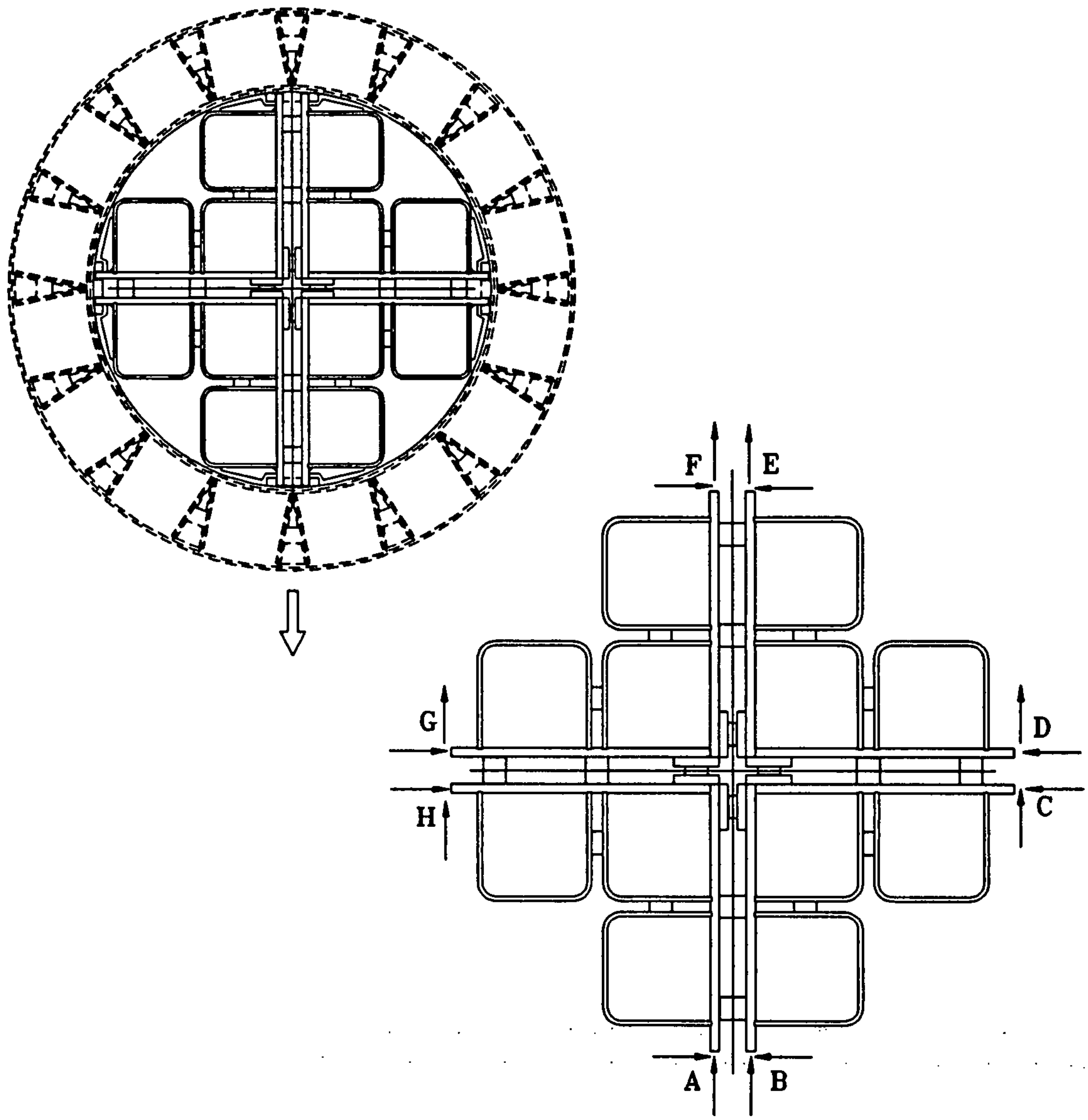

Figure 8.2-15
CASTOR X/28 Basket Tip-Over Reactions
0°-Basket Orientation

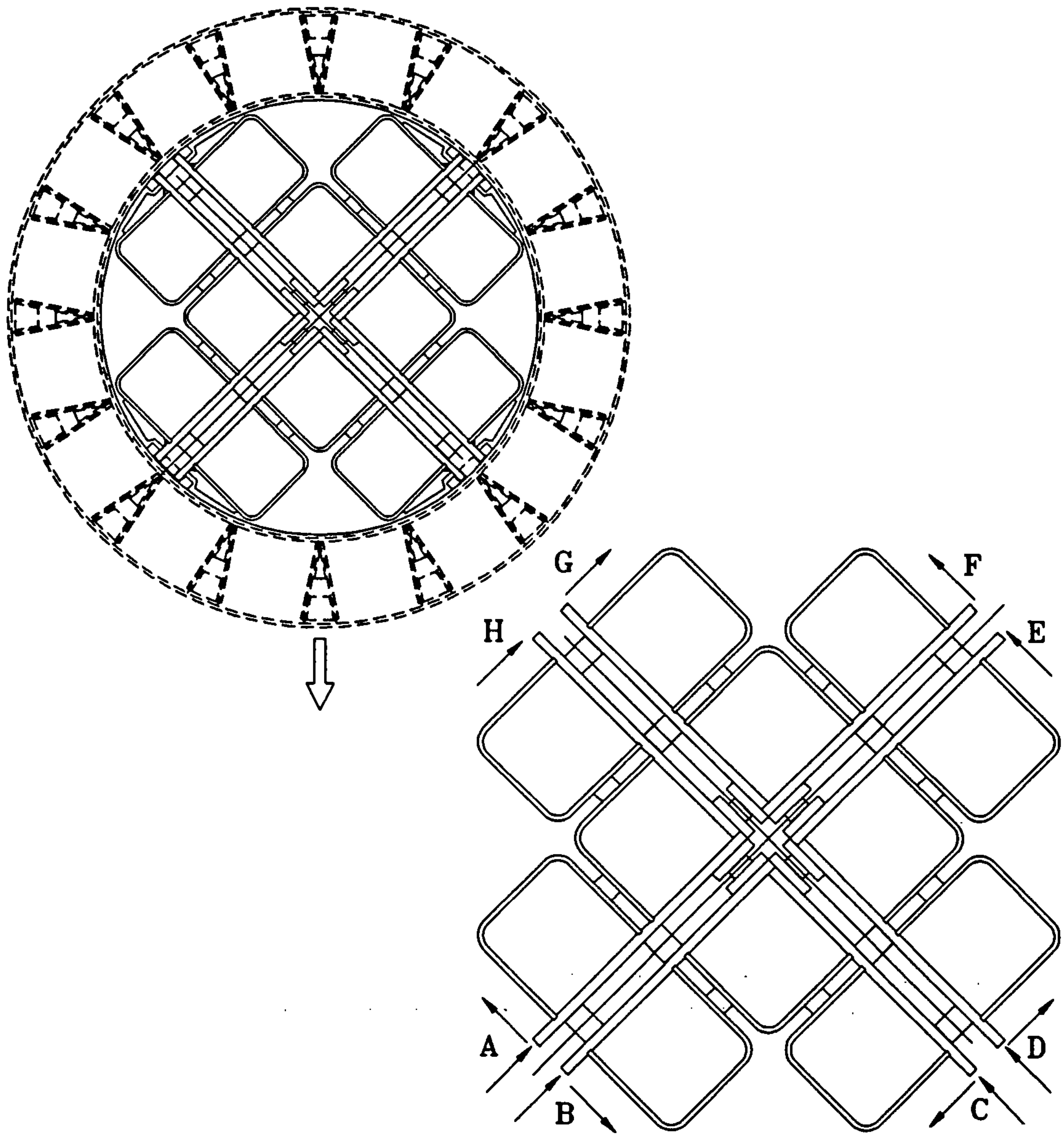

Figure 8.2-16
CASTOR X/28 Basket Tip-Over Reactions
45°-Basket Orientation

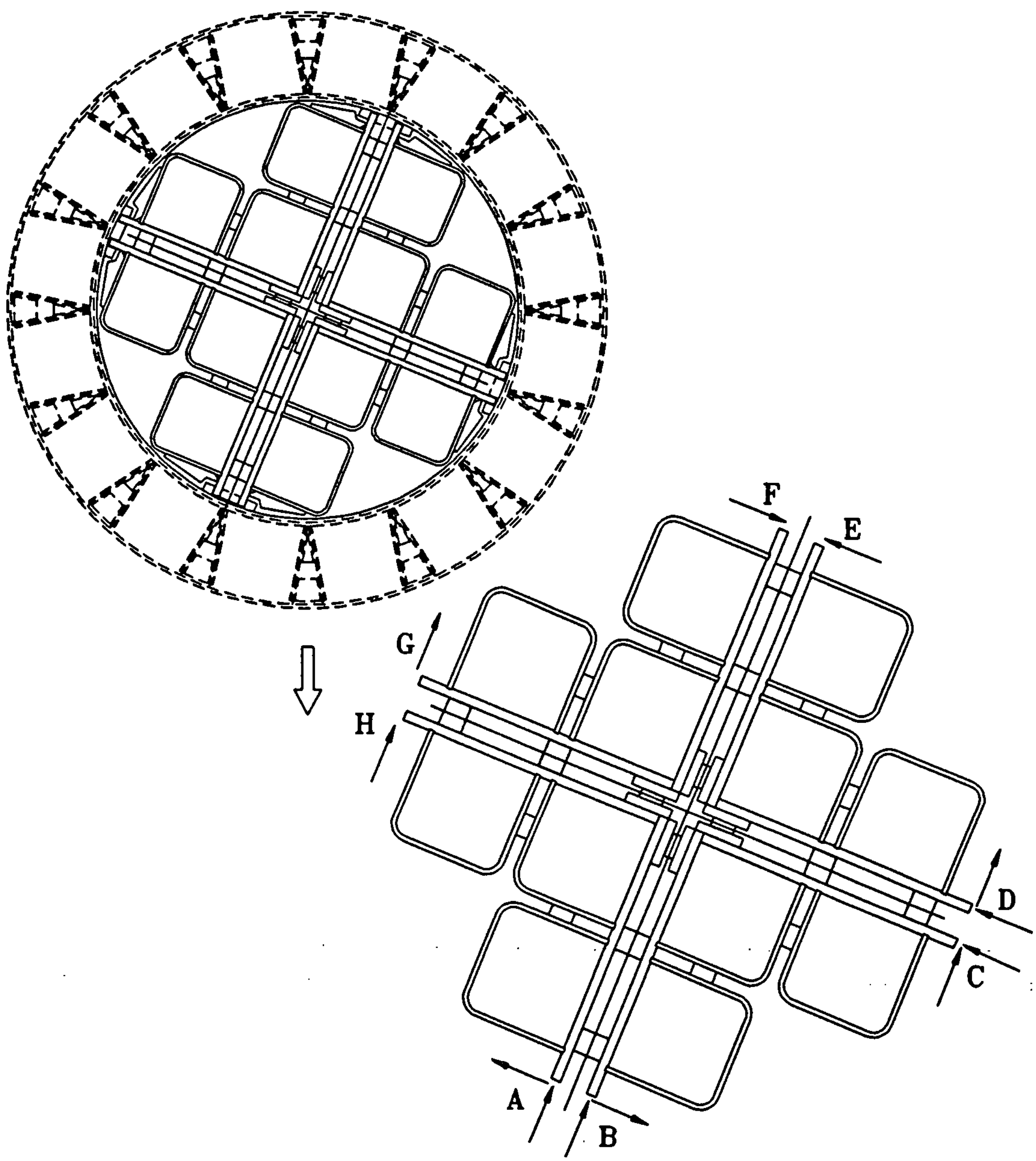

Figure 8.2-17
CASTOR X/28 Basket Tip-Over Reactions
67½°-Basket Orientation

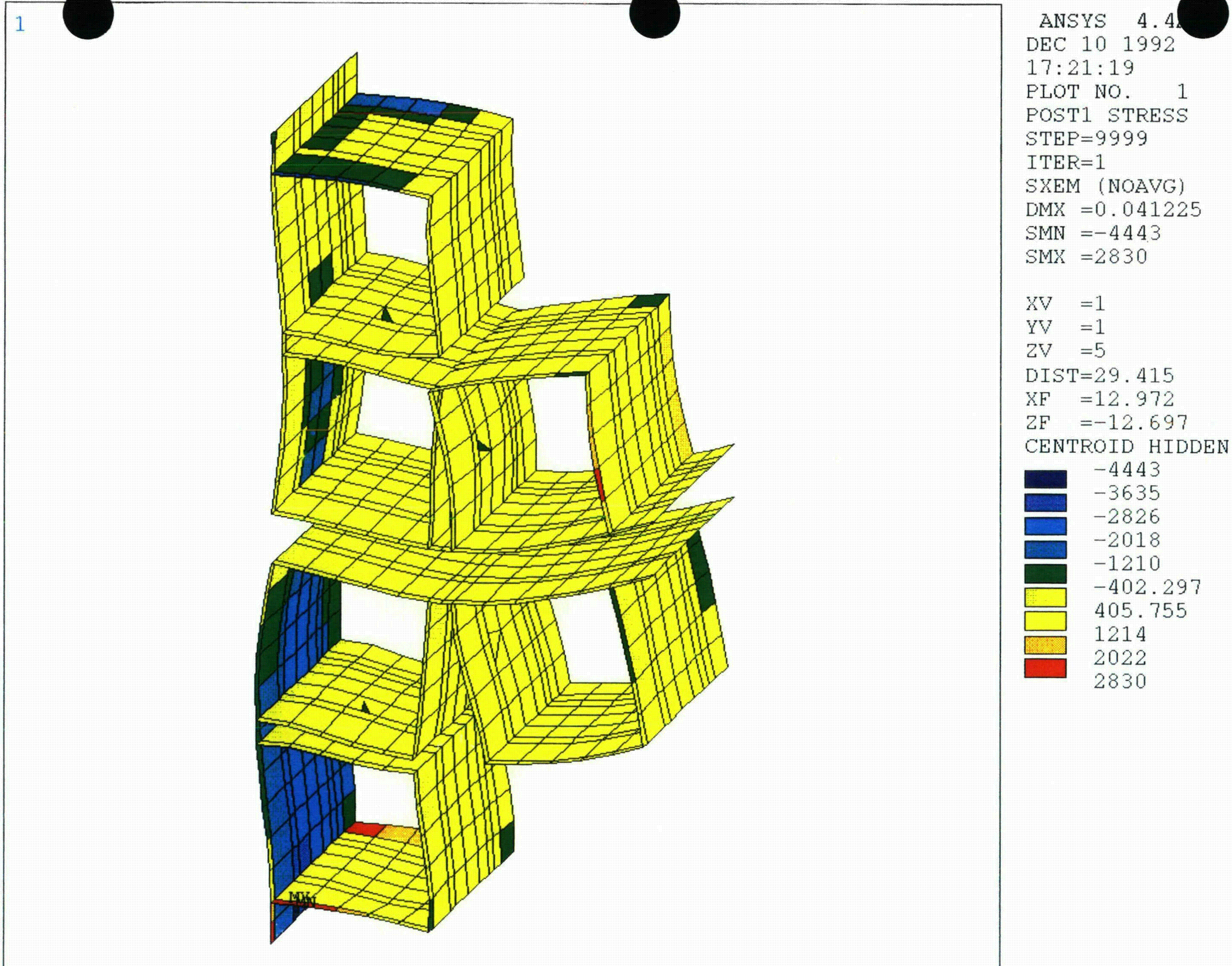

Castor X/28 - Internal Structure - 24g Side Drop (Membrane)

FIGURE 8.2 - 18

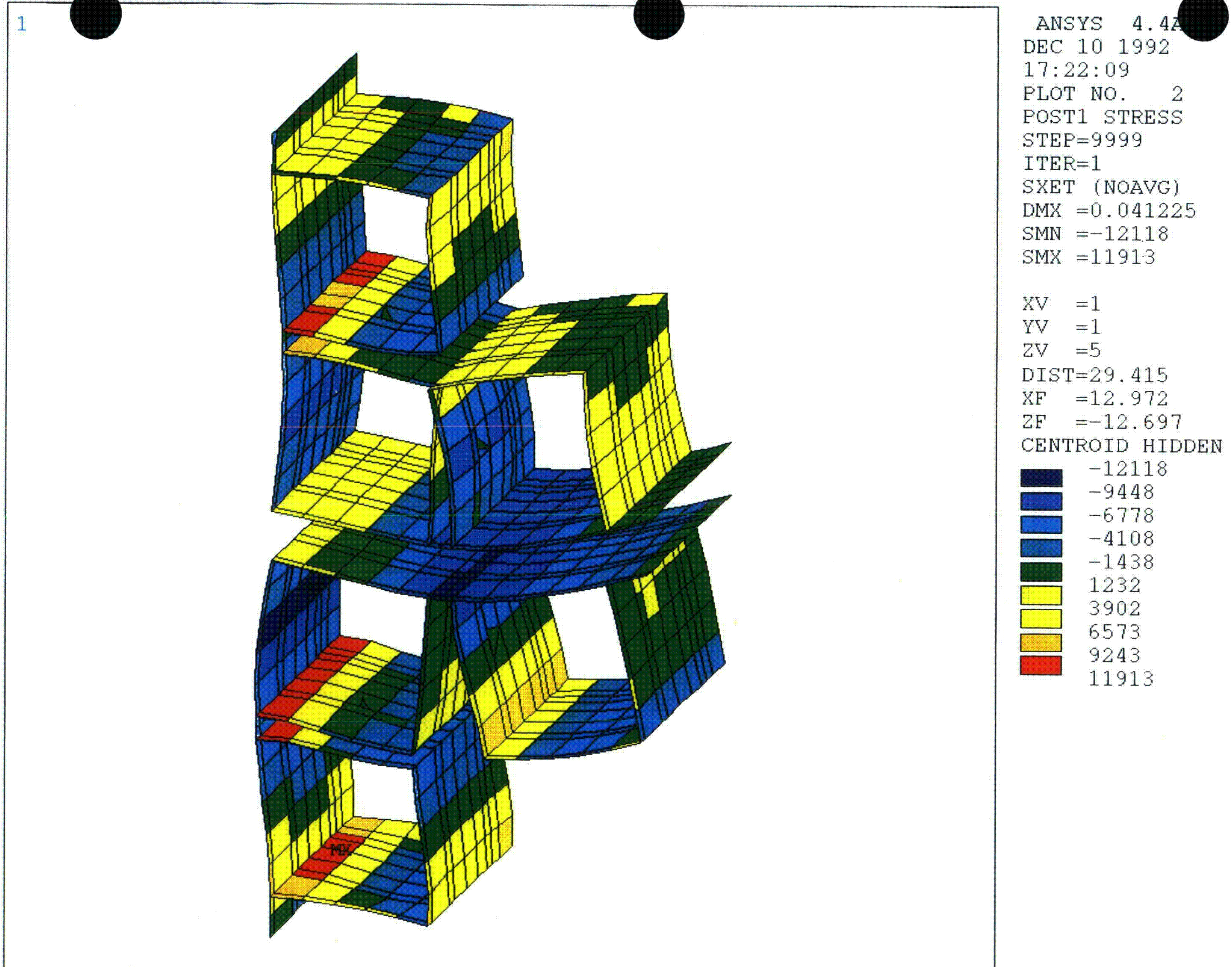

Castor X/28 - Internal Structure - 24g Side Drop (Top M + B)

FIGURE 8.2 - 19

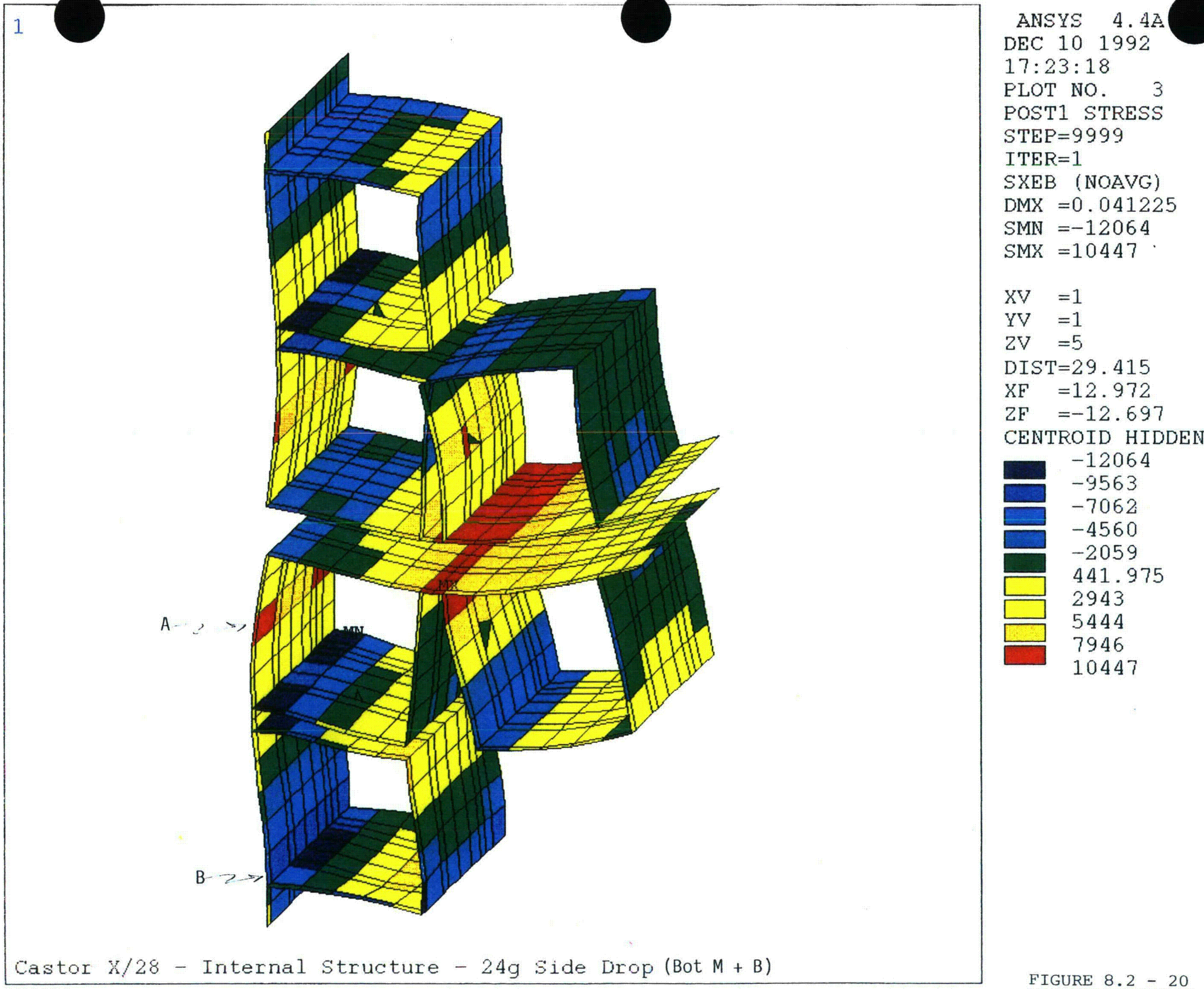
1
ANSYS 4.4A
DEC 10 1992
17:23:18
PLOT NO. 3
POST1 STRESS
STEP=9999
ITER=1
SXEB (NOAVG)
DMX =0.041225
SMN =-12064
SMX =10447
XV =1
YV =1
ZV =5
DIST=29.415
XF =12.972
ZF =-12.697
CENTROID HIDDEN
-12064
-9563
-7062
-4560
-2059
441.975
2943
5444
7946
10447
MX
MN
A
B
Castor X/28 - Internal Structure - 24g Side Drop (Bot M + B)

FIGURE 8.2 - 20

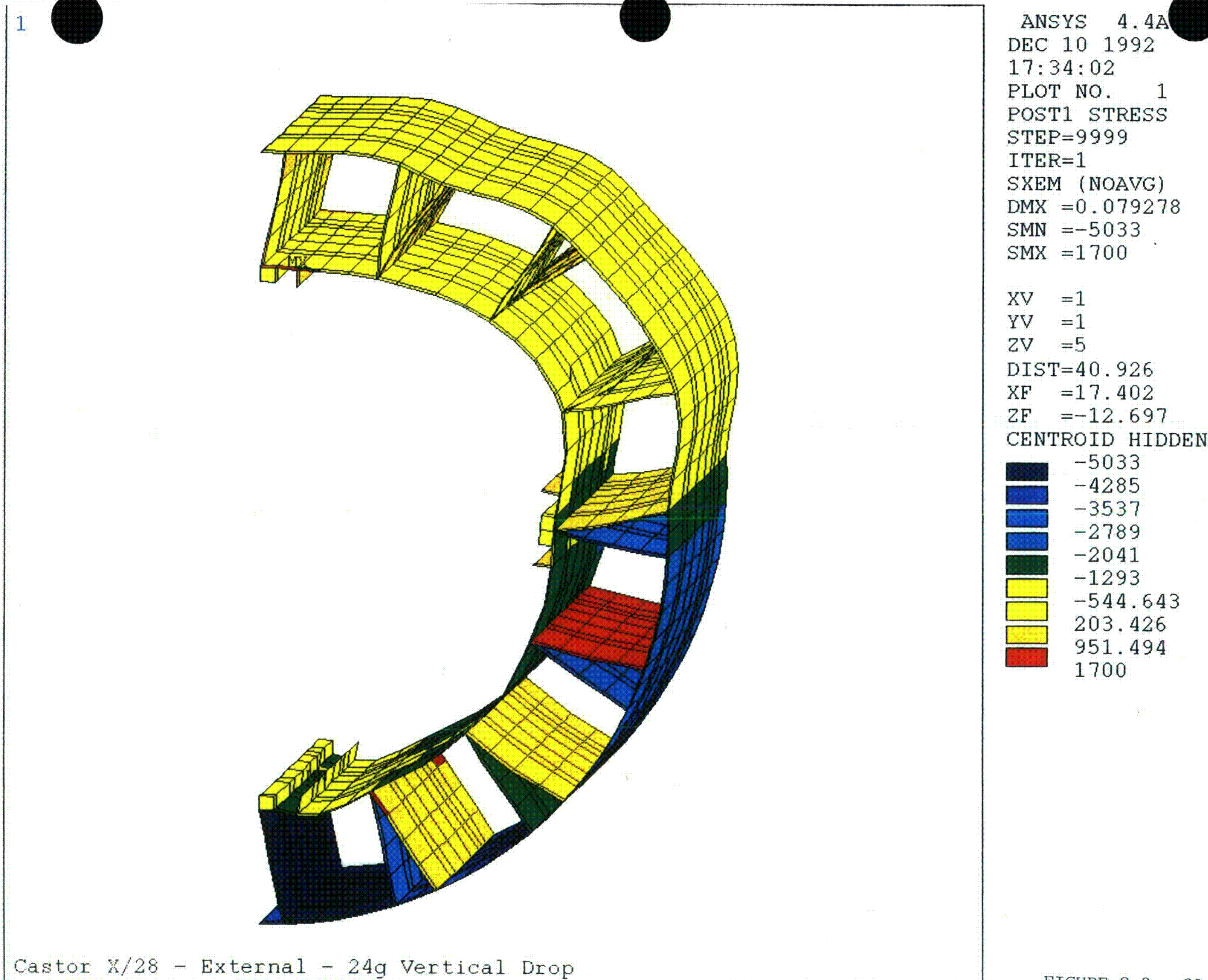
1
ANSYS 4.4A
DEC 10 1992
17:34:02
PLOT NO. 1
POST1 STRESS
STEP=9999
ITER=1
SXEM (NOAVG)
DMX =0.079278
SMN =-5033
SMX =1700
XV =1
YV =1
ZV =5
DIST=40.926
XF =17.402
ZF =-12.697
CENTROID HIDDEN
-5033
-4285
-3537
-2789
-2041
-1293
-544.643
203.426
951.494
1700
Castor X/28 - External - 24g Vertical Drop

FIGURE 8.2 - 21

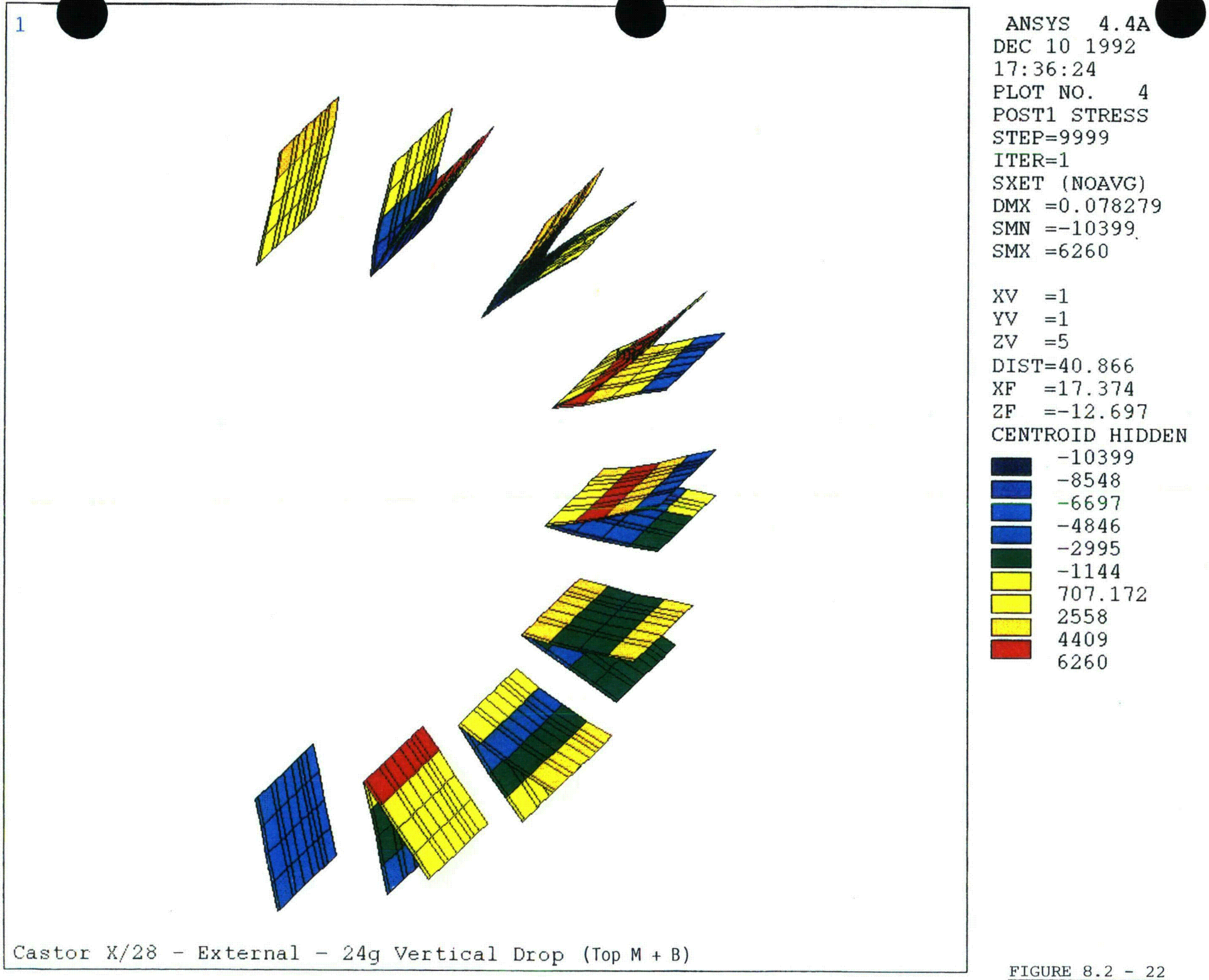
1
ANSYS 4.4A
DEC 10 1992
17:36:24
PLOT NO. 4
POST1 STRESS
STEP=9999
ITER=1
SXET (NOAVG)
DMX =0.078279
SMN =-10399
SMX =6260
XV =1
YV =1
ZV =5
DIST=40.866
XF =17.374
ZF =-12.697
CENTROID HIDDEN
-10399
-8548
-6697
-4846
-2995
-1144
707.172
2558
4409
6260
Castor X/28 - External - 24g Vertical Drop (Top M + B)

FIGURE 8.2 - 22

1

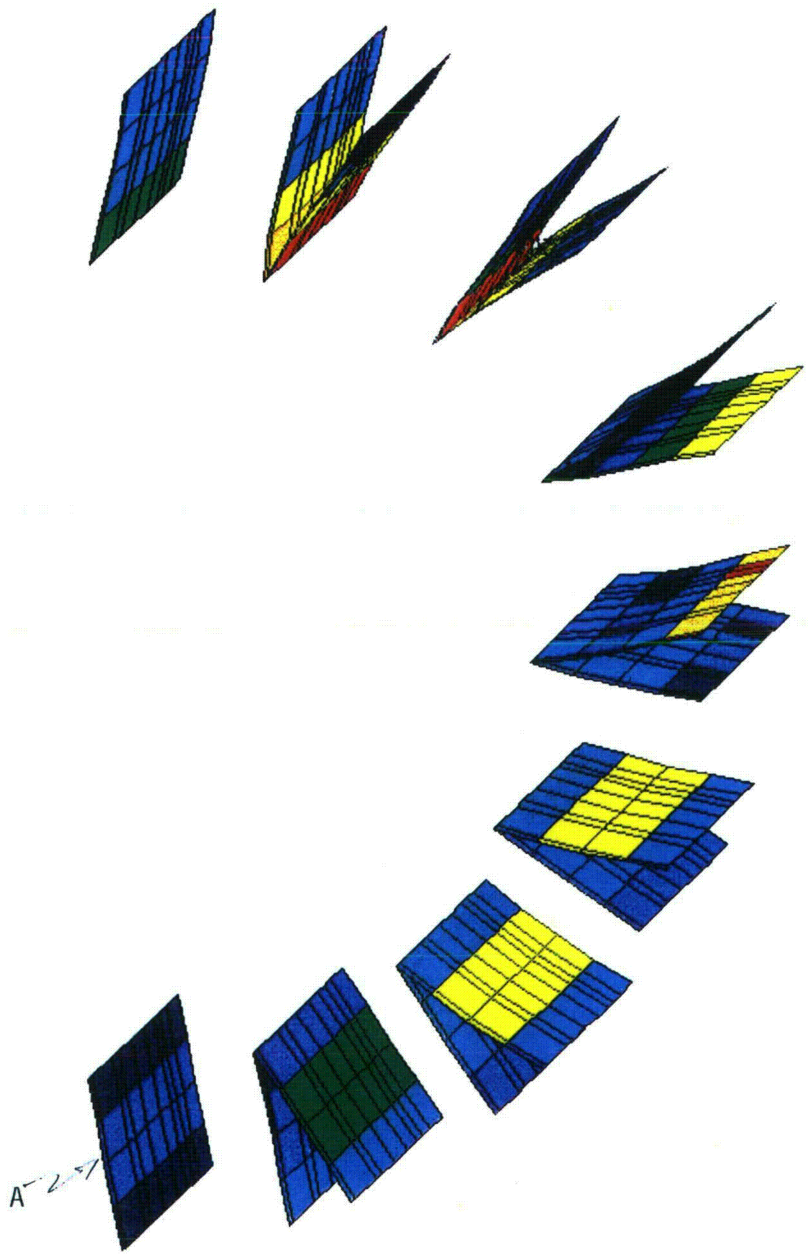

ANSYS 4.4A
DEC 10 1992
17:35:56
PLOT NO. 3
POST1 STRESS
STEP=9999
ITER=1
SXEB (NOAVG)
DMX =0.078279
SMN =-6245
SMX =9698

XV =1
YV =1
ZV =5
DIST=40.866
XF =17.374
ZF =-12.697
CENTROID HIDDEN

-6245
-4474
-2703
-931.027
840.455
2612
4383
6155
7926
9698

Castor X/28 - External - 24g Vertical Drop (Bottom M + B)

FIGURE 8.2 - 23

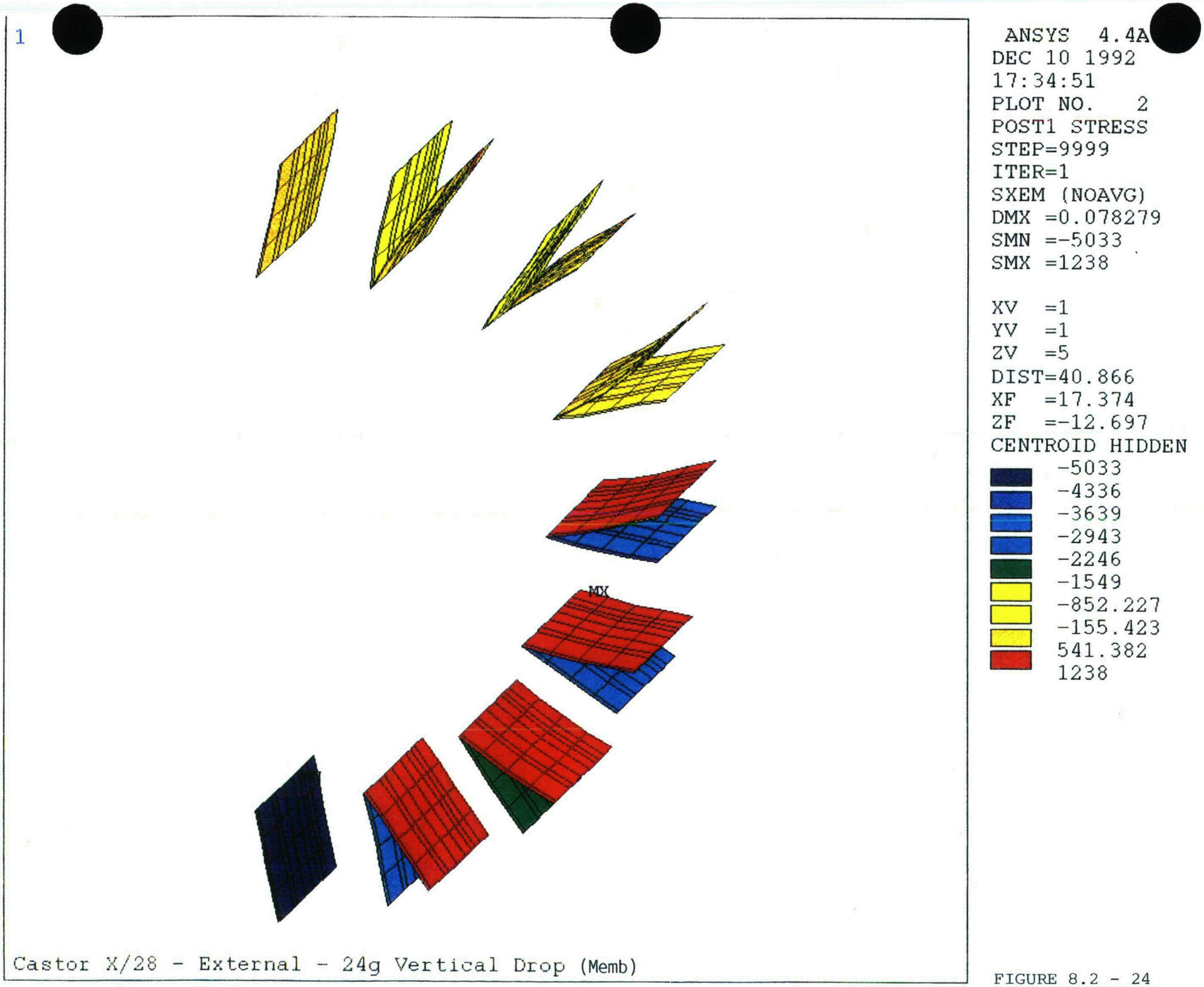
1
MX
Castor X/28 - External - 24g Vertical Drop (Memb)
ANSYS 4.4A
DEC 10 1992
17:34:51
PLOT NO. 2
POST1 STRESS
STEP=9999
ITER=1
SXEM (NOAVG)
DMX =0.078279
SMN =-5033
SMX =1238
XV =1
YV =1
ZV =5
DIST=40.866
XF =17.374
ZF =-12.697
CENTROID HIDDEN
-5033
-4336
-3639
-2943
-2246
-1549
-852.227
-155.423
541.382
1238

FIGURE 8.2 - 24

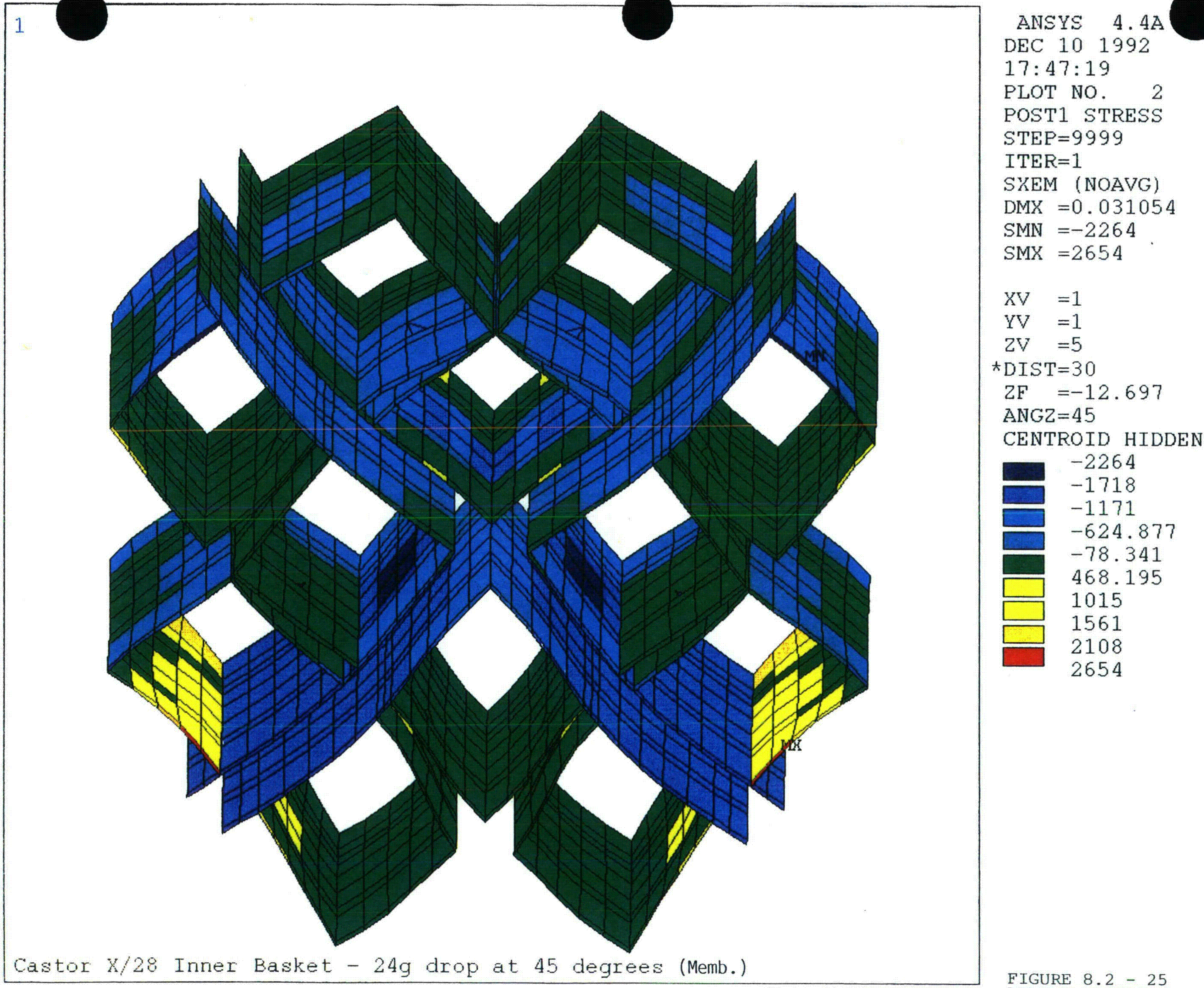
1
ANSYS 4.4A
DEC 10 1992
17:47:19
PLOT NO. 2
POST1 STRESS
STEP=9999
ITER=1
SXEM (NOAVG)
DMX =0.031054
SMN =-2264
SMX =2654
XV =1
YV =1
ZV =5
*DIST=30
ZF =-12.697
ANGZ=45
CENTROID HIDDEN
-2264
-1718
-1171
-624.877
-78.341
468.195
1015
1561
2108
2654
MN
MX
Castor X/28 Inner Basket - 24g drop at 45 degrees (Memb.)

FIGURE 8.2 - 25

1

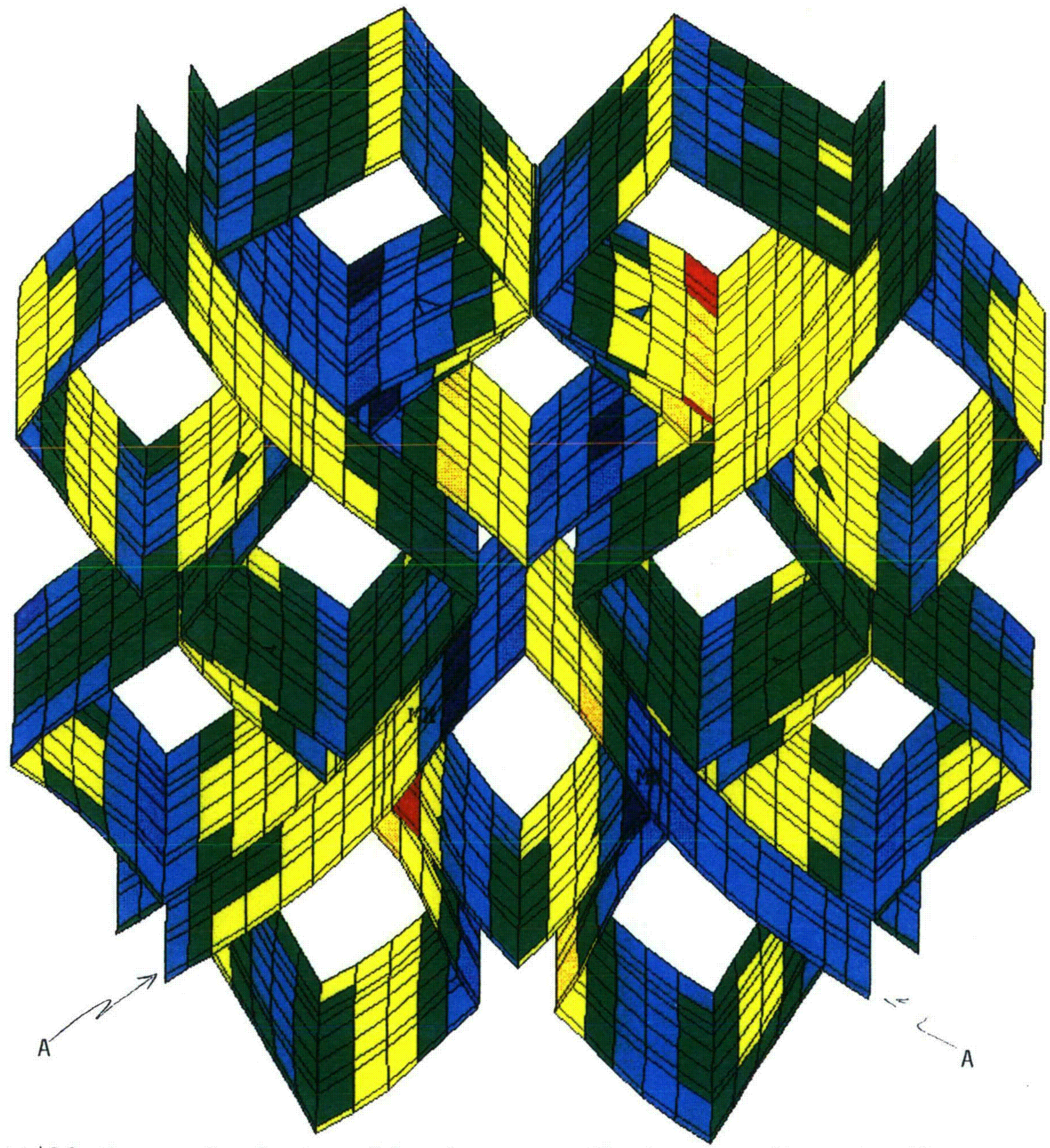

ANSYS 4.4A
DEC 10 1992
17:48:39
PLOT NO. 4
POST1 STRESS
STEP=9999
ITER=1
SXEB (NOAVG)
DMX =0.031054
SMN =-10633
SMX =11235

XV =1
YV =1
ZV =5
*DIST=30
ZF =-12.697
ANGZ=45
CENTROID HIDDEN

-10633
-8203
-5773
-3343
-913.599
1516
3946
6376 ←
8806
11235

Castor X/28 Inner Basket - 24g drop at 45 degrees (Bot. M + B)

FIGURE 8.2 - 26

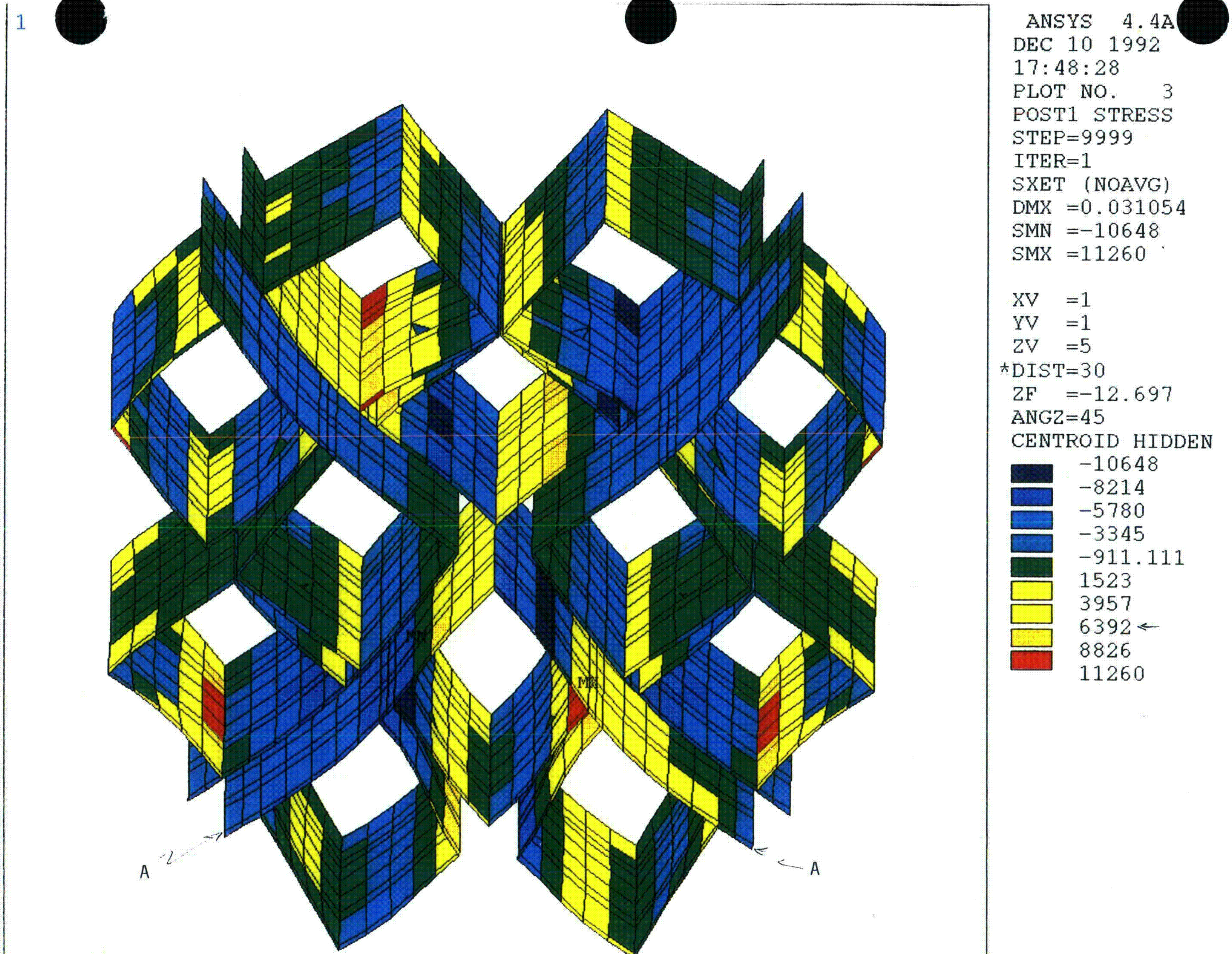

Castor X/28 Inner Basket - 24g drop at 45 degrees (Top M + B)

FIGURE 8.2 - 27

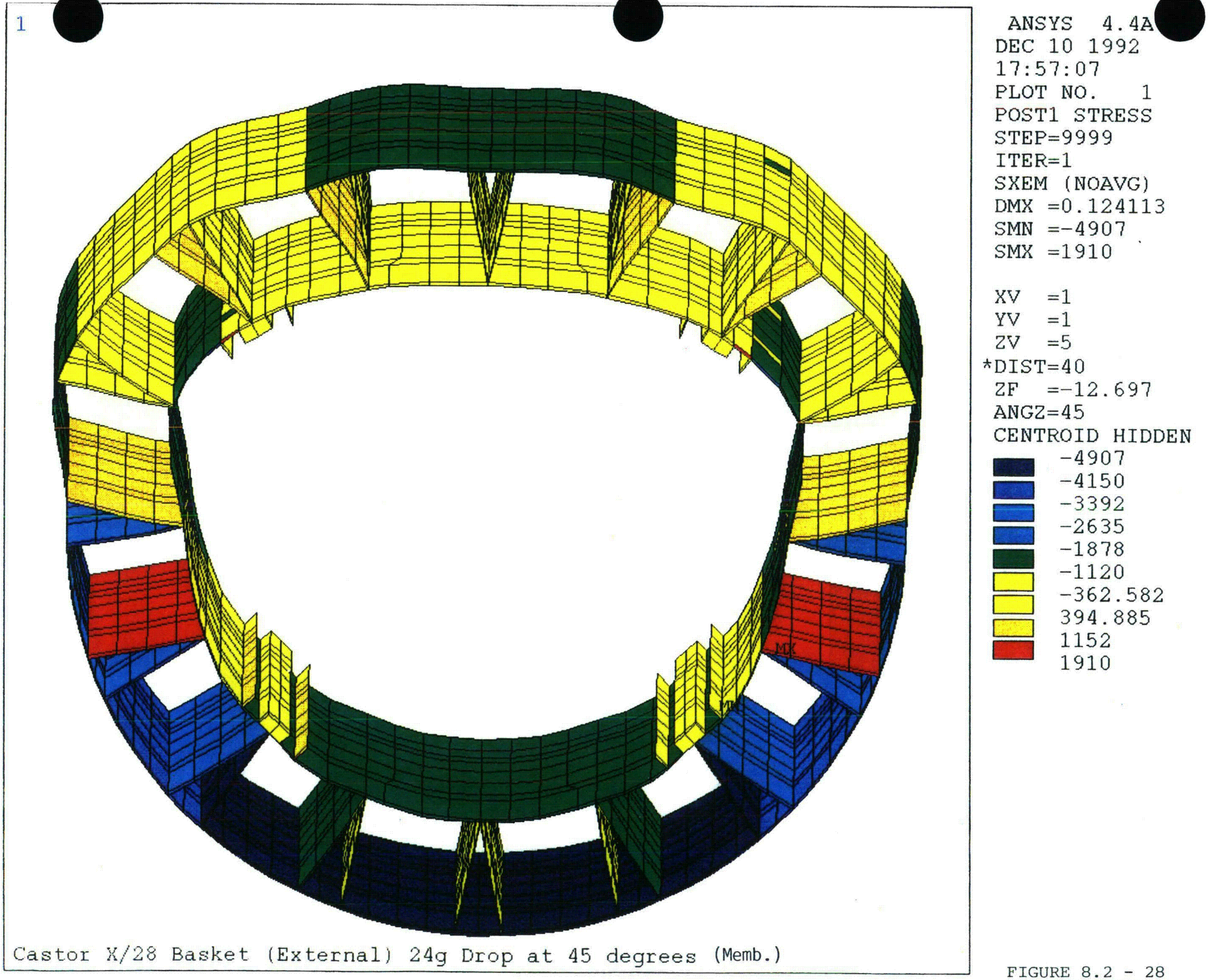
1
ANSYS 4.4A
DEC 10 1992
17:57:07
PLOT NO. 1
POST1 STRESS
STEP=9999
ITER=1
SXEM (NOAVG)
DMX =0.124113
SMN =-4907
SMX =1910
XV =1
YV =1
ZV =5
*DIST=40
ZF =-12.697
ANGZ=45
CENTROID HIDDEN
-4907
-4150
-3392
-2635
-1878
-1120
-362.582
394.885
1152
1910
Castor X/28 Basket (External) 24g Drop at 45 degrees (Memb.)

FIGURE 8.2 - 28

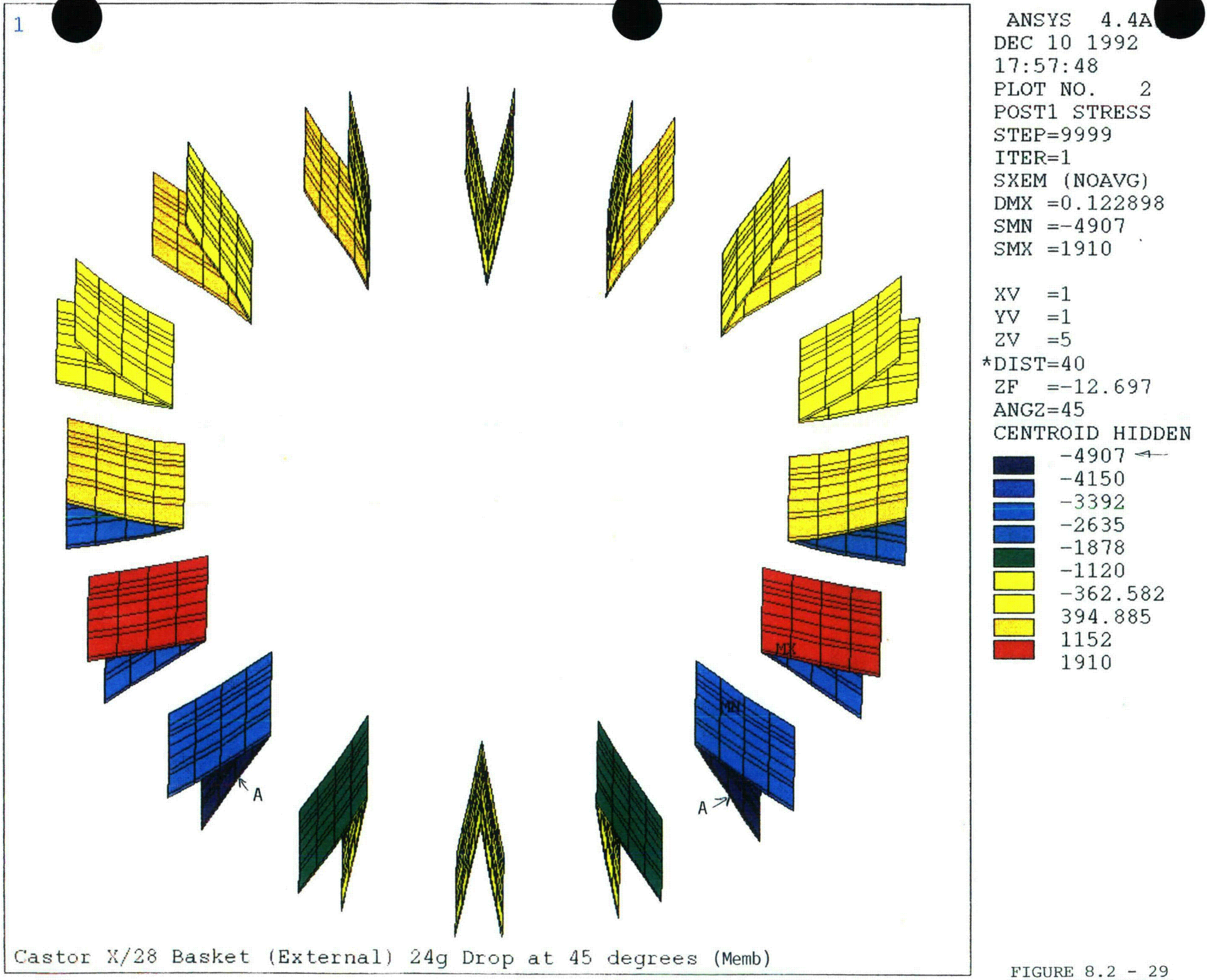
1
A
A
MX
MN
Castor X/28 Basket (External) 24g Drop at 45 degrees (Memb)
ANSYS 4.4A
DEC 10 1992
17:57:48
PLOT NO. 2
POST1 STRESS
STEP=9999
ITER=1
SXEM (NOAVG)
DMX =0.122898
SMN =-4907
SMX =1910
XV =1
YV =1
ZV =5
*DIST=40
ZF =-12.697
ANGZ=45
CENTROID HIDDEN
-4907
-4150
-3392
-2635
-1878
-1120
-362.582
394.885
1152
1910

FIGURE 8.2 - 29

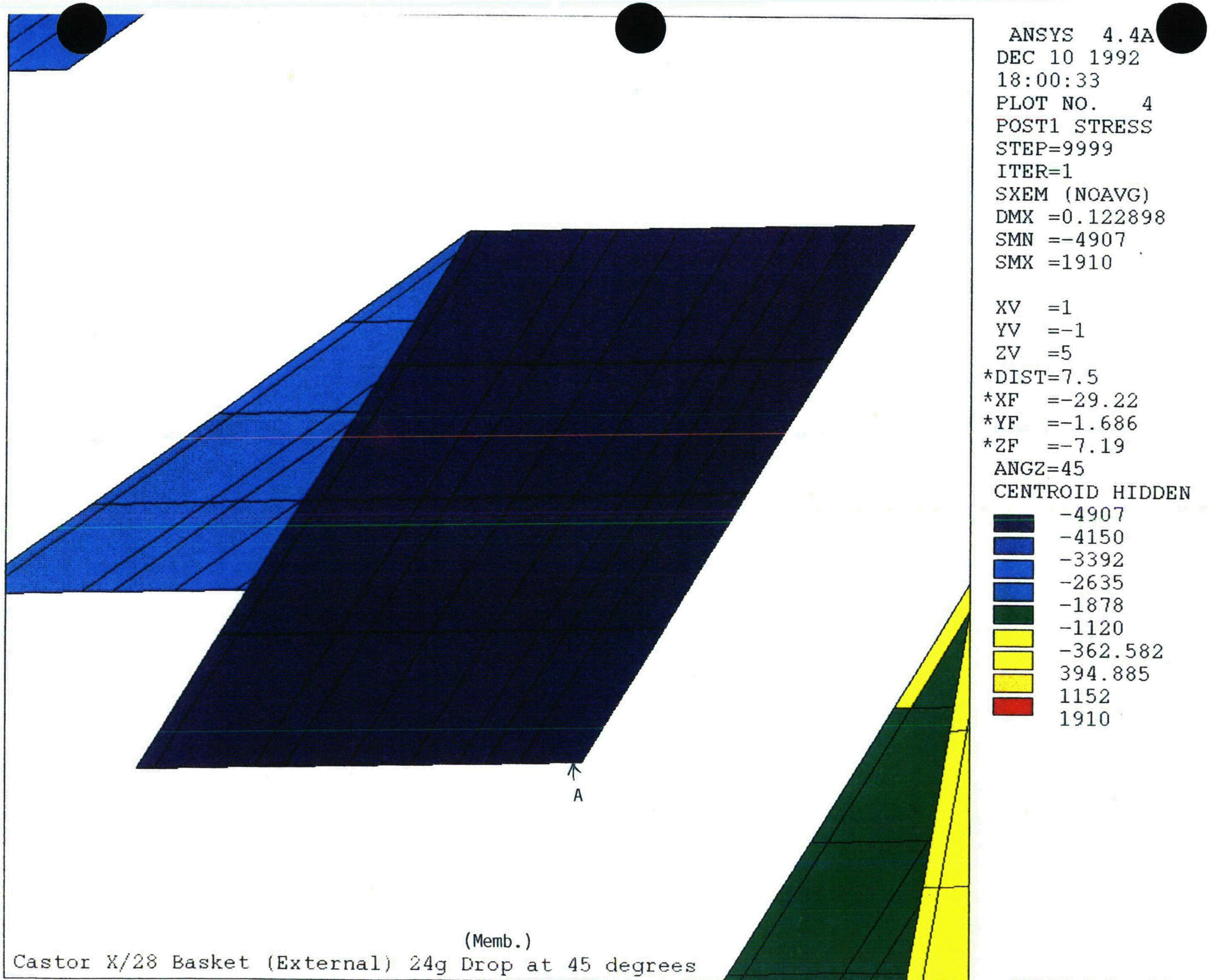
ANSYS 4.4A
DEC 10 1992
18:00:33
PLOT NO. 4
POST1 STRESS
STEP=9999
ITER=1
SXEM (NOAVG)
DMX =0.122898
SMN =-4907
SMX =1910
XV =1
YV =-1
ZV =5
*DIST=7.5
*XF =-29.22
*YF =-1.686
*ZF =-7.19
ANGZ=45
CENTROID HIDDEN
-4907
-4150
-3392
-2635
-1878
-1120
-362.582
394.885
1152
1910
A
(Memb.)
Castor X/28 Basket (External) 24g Drop at 45 degrees

FIGURE 8.2 - 30

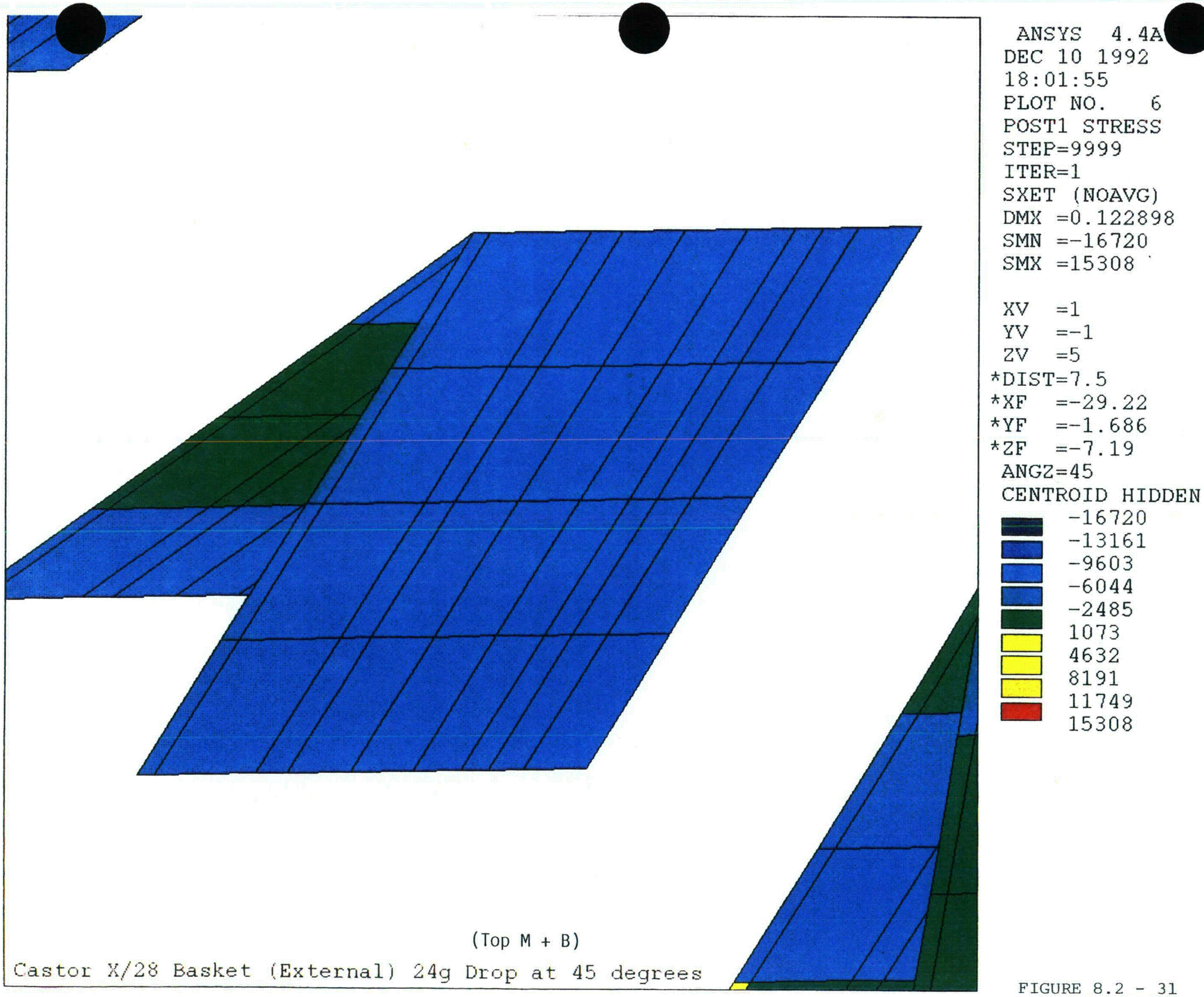
ANSYS 4.4A
DEC 10 1992
18:01:55
PLOT NO. 6
POST1 STRESS
STEP=9999
ITER=1
SXET (NOAVG)
DMX =0.122898
SMN =-16720
SMX =15308
XV =1
YV =-1
ZV =5
*DIST=7.5
*XF =-29.22
*YF =-1.686
*ZF =-7.19
ANGZ=45
CENTROID HIDDEN
-16720
-13161
-9603
-6044
-2485
1073
4632
8191
11749
15308
(Top M + B)
Castor X/28 Basket (External) 24g Drop at 45 degrees

FIGURE 8.2 - 31

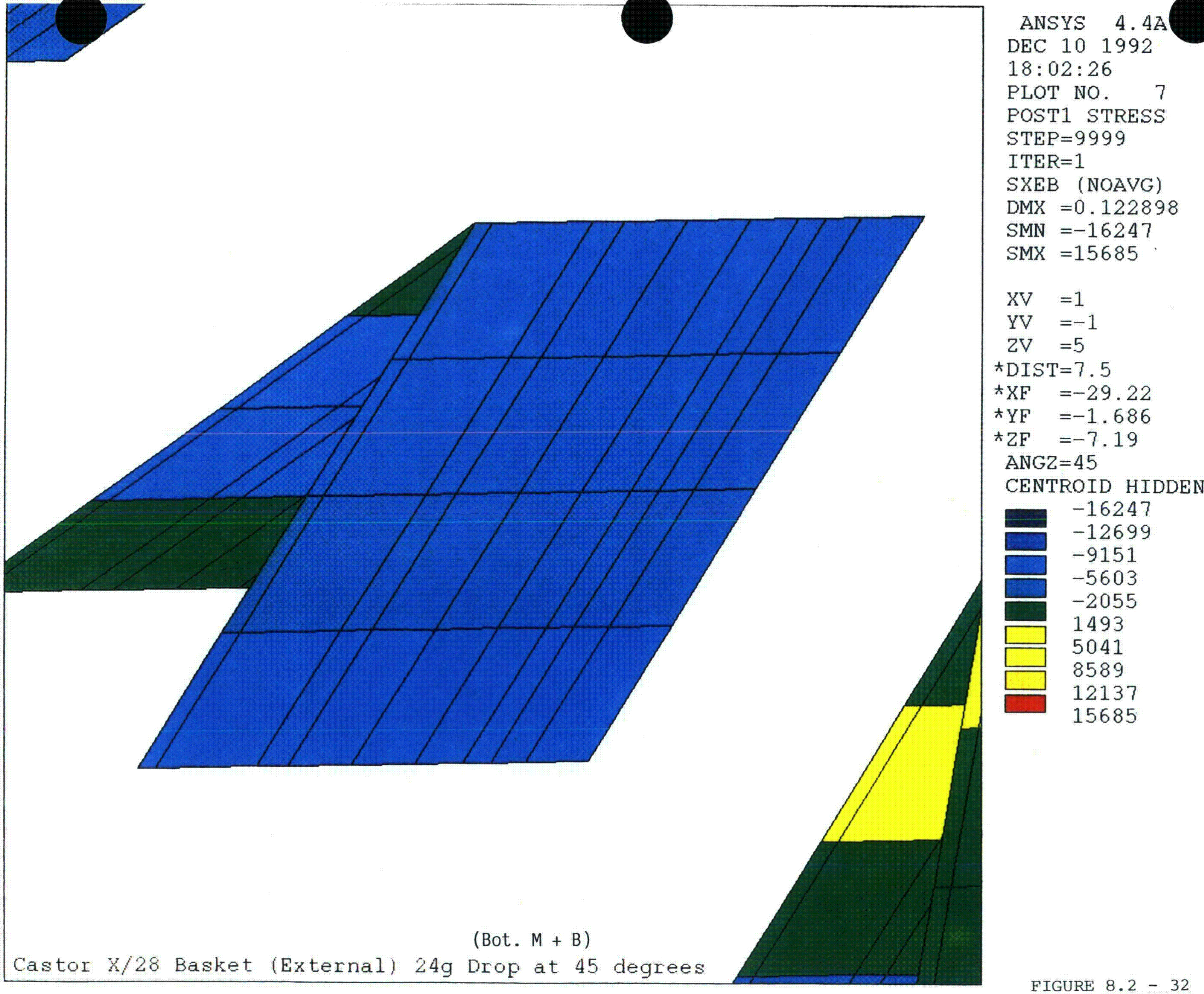
ANSYS 4.4A
DEC 10 1992
18:02:26
PLOT NO. 7
POST1 STRESS
STEP=9999
ITER=1
SXEB (NOAVG)
DMX =0.122898
SMN =-16247
SMX =15685
XV =1
YV =-1
ZV =5
*DIST=7.5
*XF =-29.22
*YF =-1.686
*ZF =-7.19
ANGZ=45
CENTROID HIDDEN
-16247
-12699
-9151
-5603
-2055
1493
5041
8589
12137
15685
(Bot. M + B)
Castor X/28 Basket (External) 24g Drop at 45 degrees

FIGURE 8.2 - 32

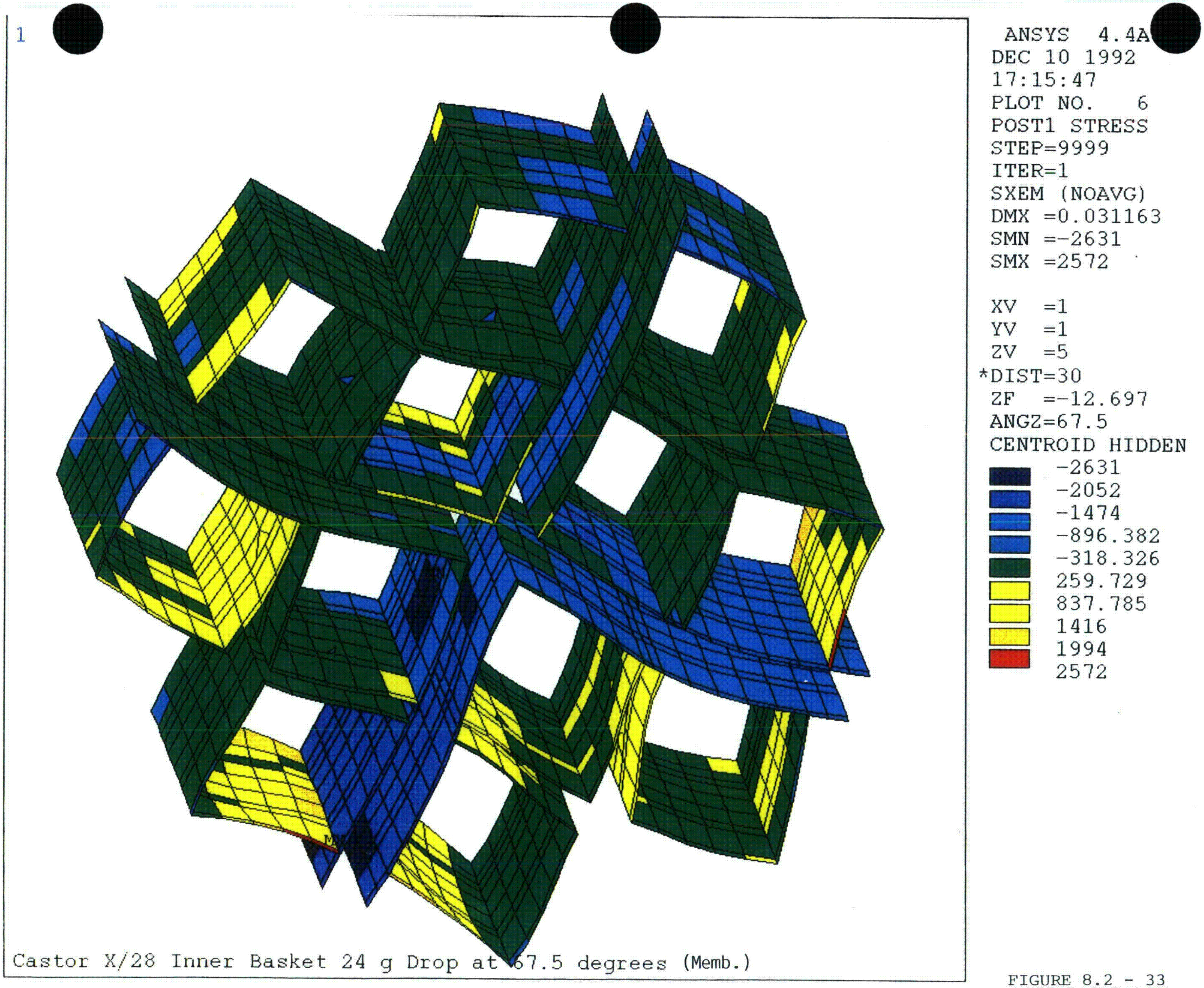
1
ANSYS 4.4A
DEC 10 1992
17:15:47
PLOT NO. 6
POST1 STRESS
STEP=9999
ITER=1
SXEM (NOAVG)
DMX =0.031163
SMN =-2631
SMX =2572
XV =1
YV =1
ZV =5
*DIST=30
ZF =-12.697
ANGZ=67.5
CENTROID HIDDEN
-2631
-2052
-1474
-896.382
-318.326
259.729
837.785
1416
1994
2572
Castor X/28 Inner Basket 24 g Drop at 67.5 degrees (Memb.)

FIGURE 8.2 - 33

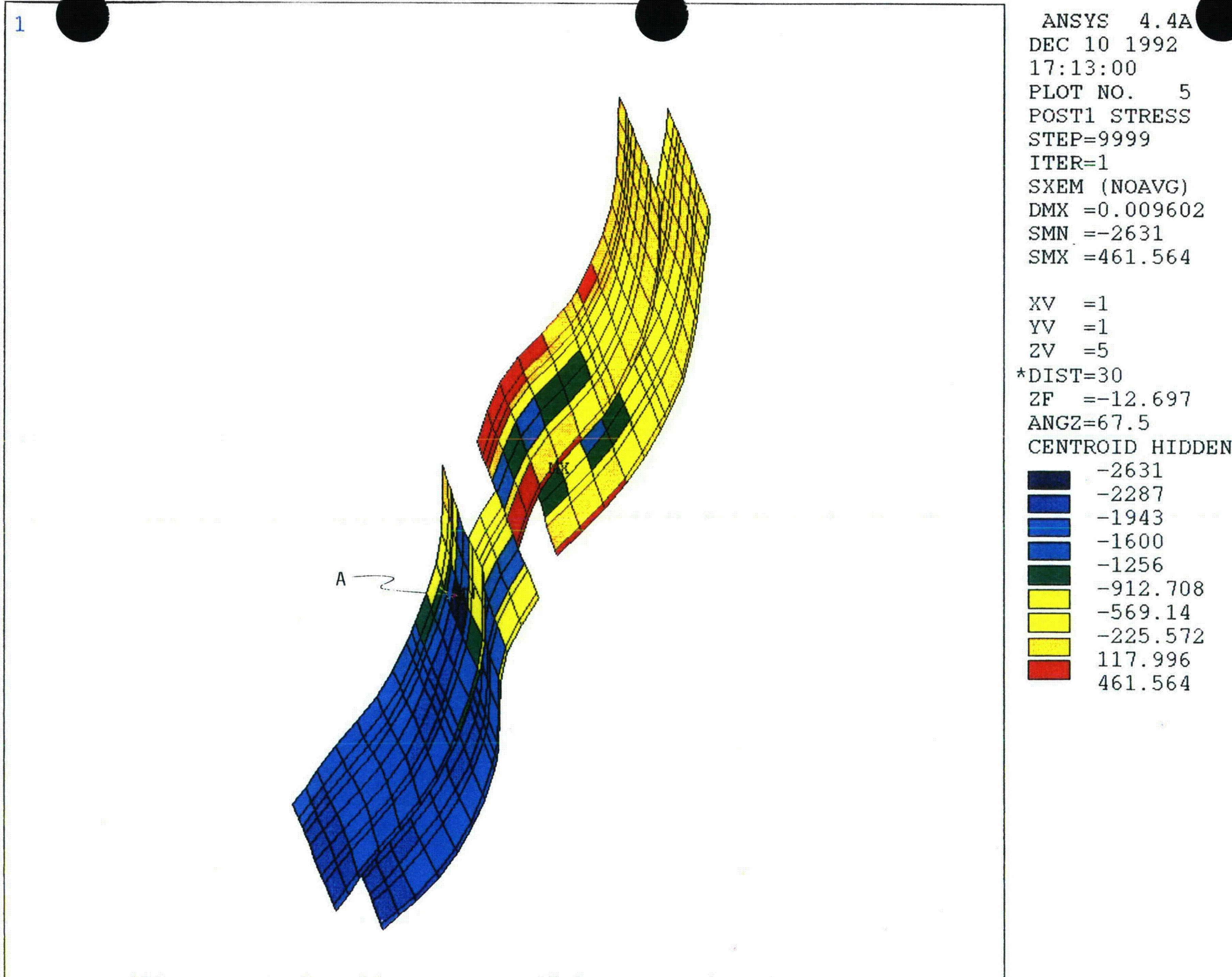

Castor X/28 Inner Basket 24 g Drop at 67.5 degrees (Memb.)

FIGURE 8.2 - 34

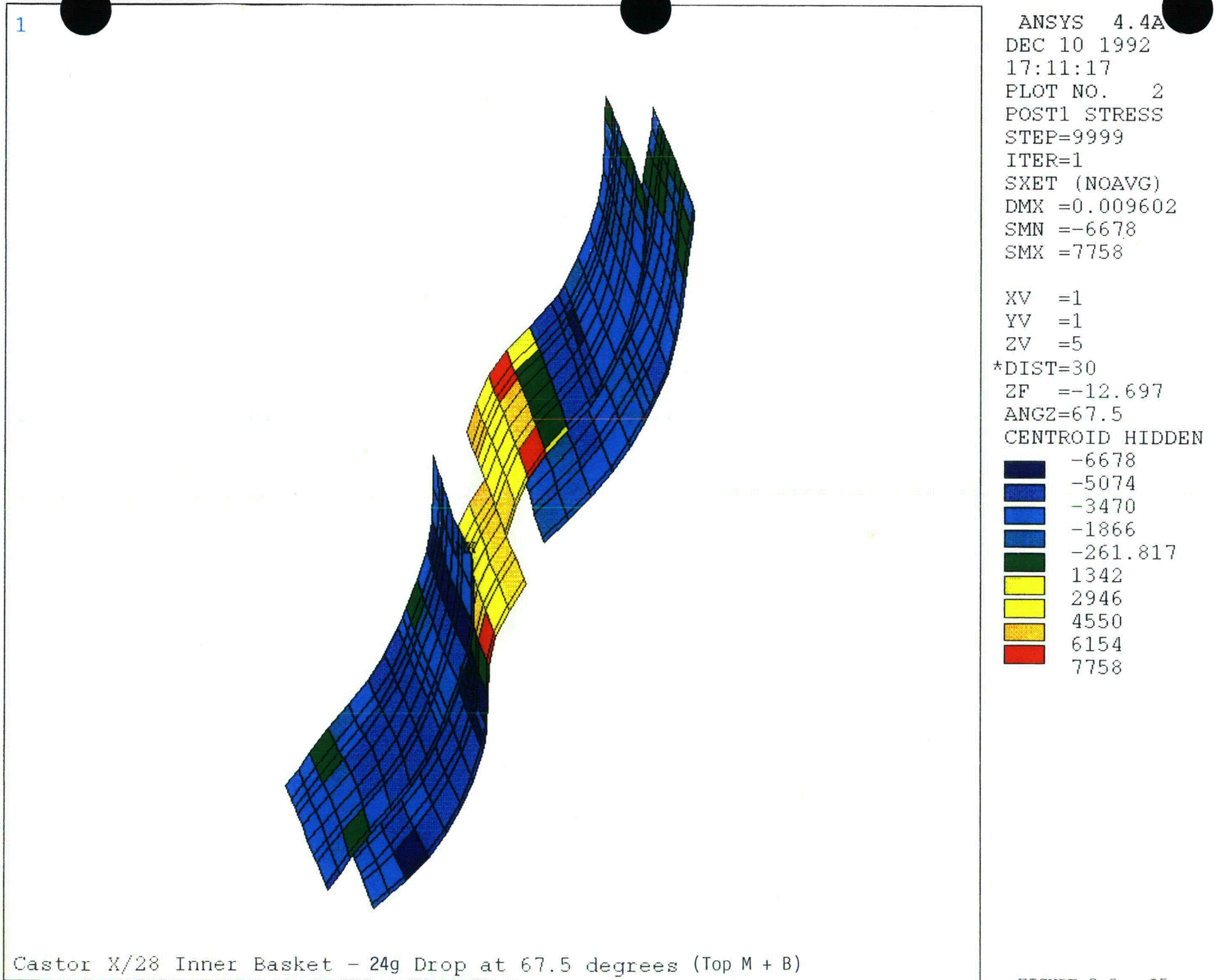

Castor X/28 Inner Basket - 24g Drop at 67.5 degrees (Top M + B)

FIGURE 8.2 - 35

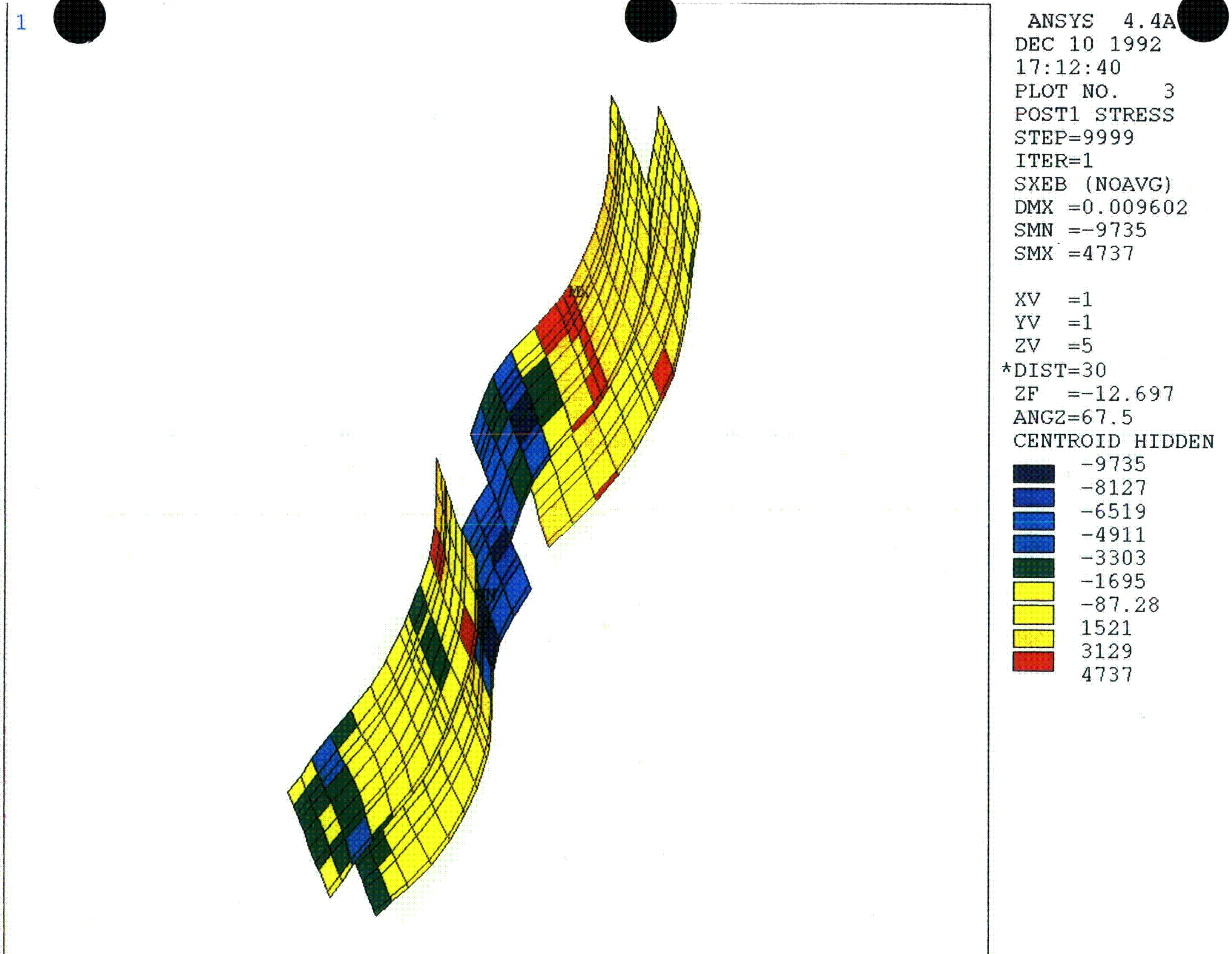

Castor X/28 Inner Basket 24 g Drop at 67.5 degrees (Bot. M + B)

FIGURE 8.2 - 36

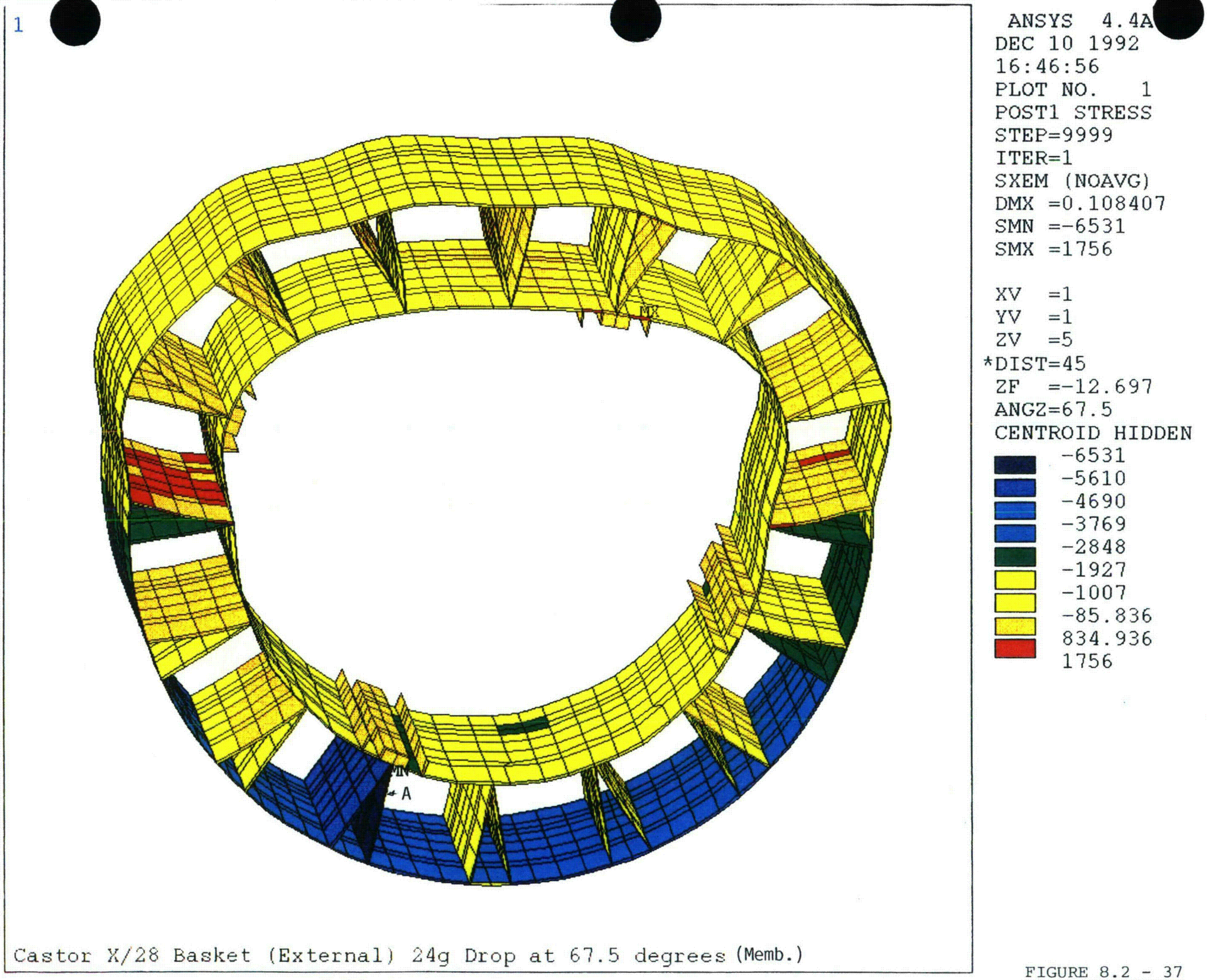
1
ANSYS 4.4A
DEC 10 1992
16:46:56
PLOT NO. 1
POST1 STRESS
STEP=9999
ITER=1
SXEM (NOAVG)
DMX =0.108407
SMN =-6531
SMX =1756
XV =1
YV =1
ZV =5
*DIST=45
ZF =-12.697
ANGZ=67.5
CENTROID HIDDEN
-6531
-5610
-4690
-3769
-2848
-1927
-1007
-85.836
834.936
1756
MX
A
Castor X/28 Basket (External) 24g Drop at 67.5 degrees (Memb.)

FIGURE 8.2 - 37

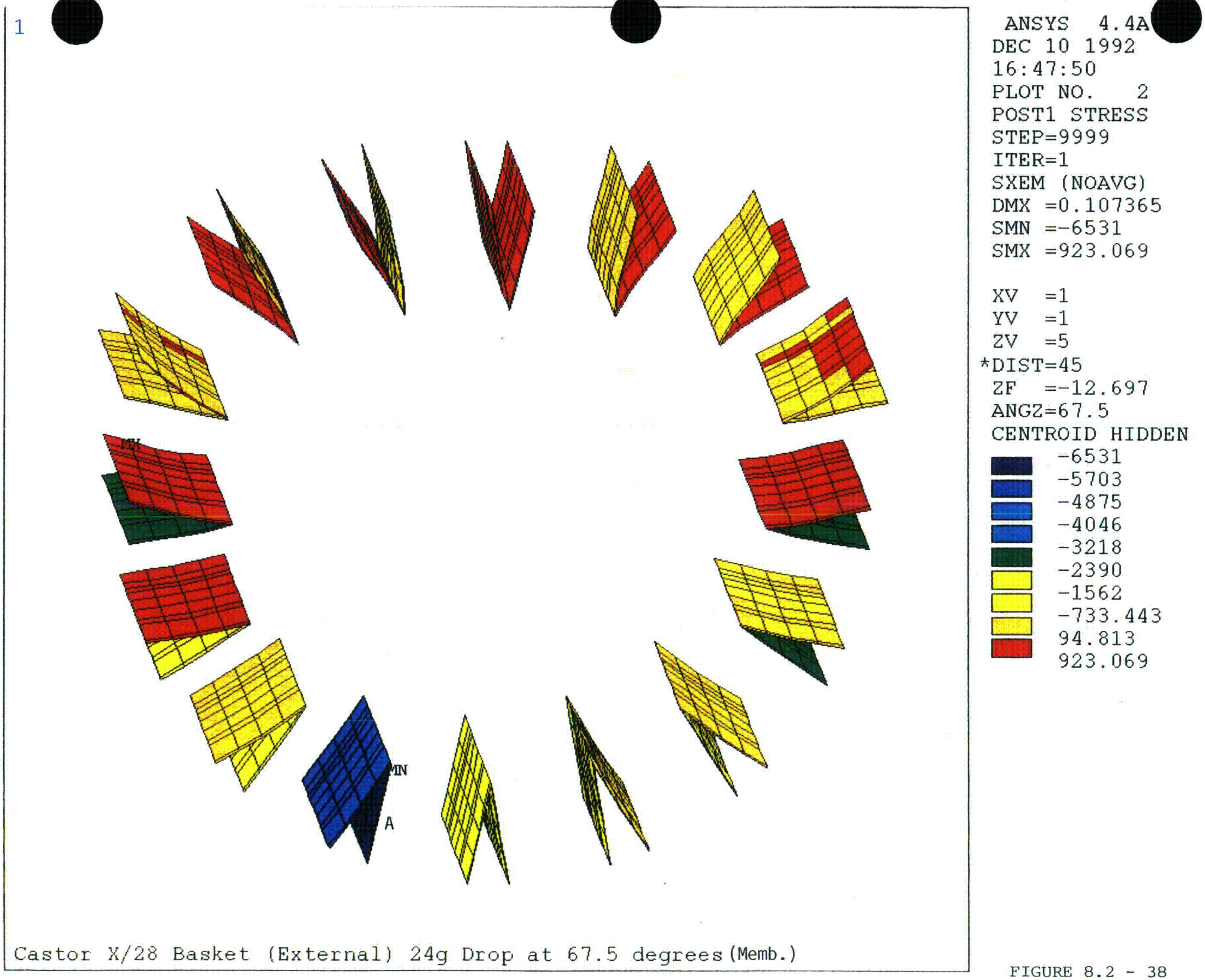
1
ANSYS 4.4A
DEC 10 1992
16:47:50
PLOT NO. 2
POST1 STRESS
STEP=9999
ITER=1
SXEM (NOAVG)
DMX =0.107365
SMN =-6531
SMX =923.069
XV =1
YV =1
ZV =5
*DIST=45
ZF =-12.697
ANGZ=67.5
CENTROID HIDDEN
-6531
-5703
-4875
-4046
-3218
-2390
-1562
-733.443
94.813
923.069
MN
A
Castor X/28 Basket (External) 24g Drop at 67.5 degrees (Memb.)

FIGURE 8.2 - 38

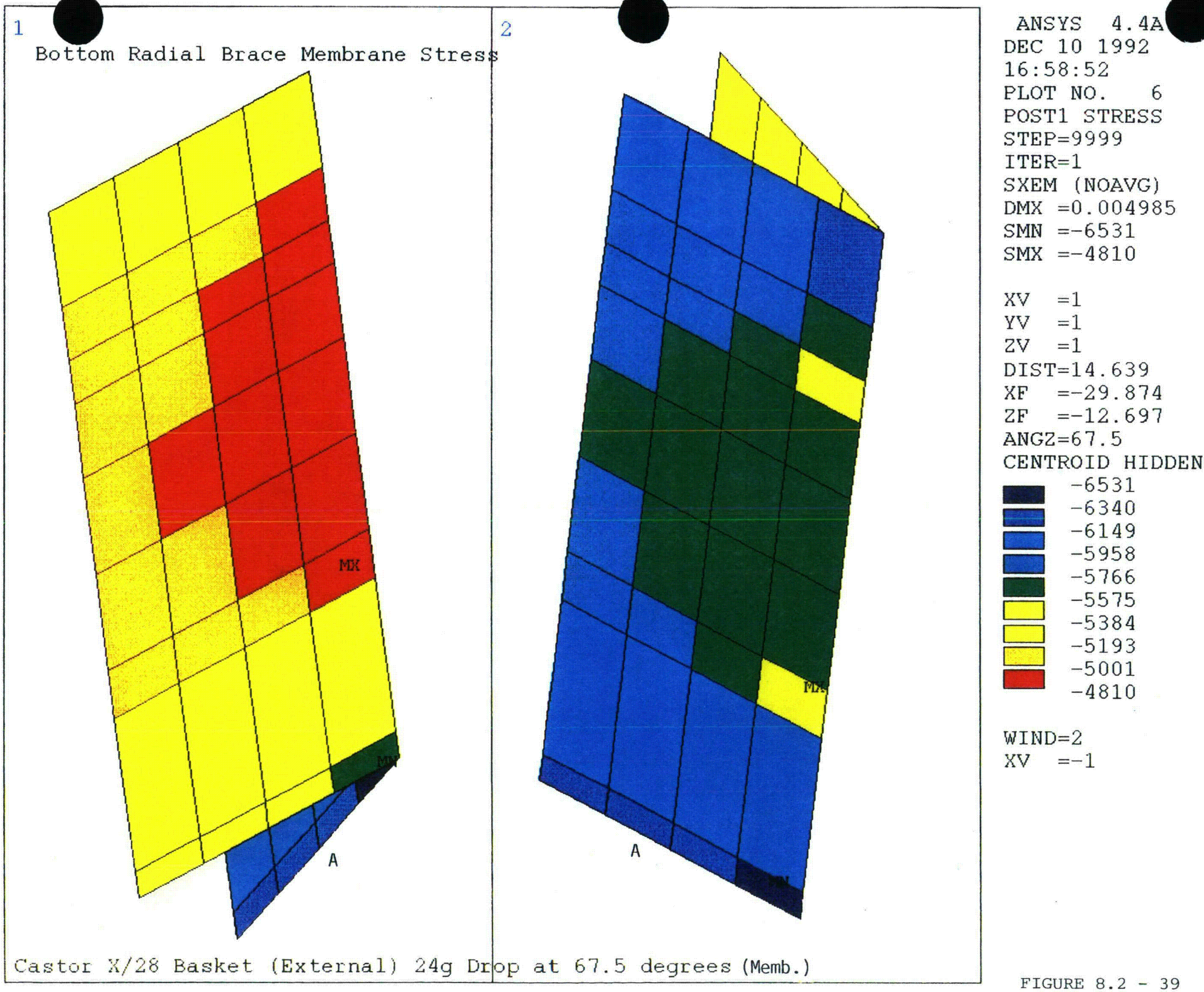
1
Bottom Radial Brace Membrane Stress
MX
MN
A
2
MX
MN
A
Castor X/28 Basket (External) 24g Drop at 67.5 degrees (Memb.)
ANSYS 4.4A
DEC 10 1992
16:58:52
PLOT NO. 6
POST1 STRESS
STEP=9999
ITER=1
SXEM (NOAVG)
DMX =0.004985
SMN =-6531
SMX =-4810
XV =1
YV =1
ZV =1
DIST=14.639
XF =-29.874
ZF =-12.697
ANGZ=67.5
CENTROID HIDDEN
-6531
-6340
-6149
-5958
-5766
-5575
-5384
-5193
-5001
-4810
WIND=2
XV =-1

FIGURE 8.2 - 39

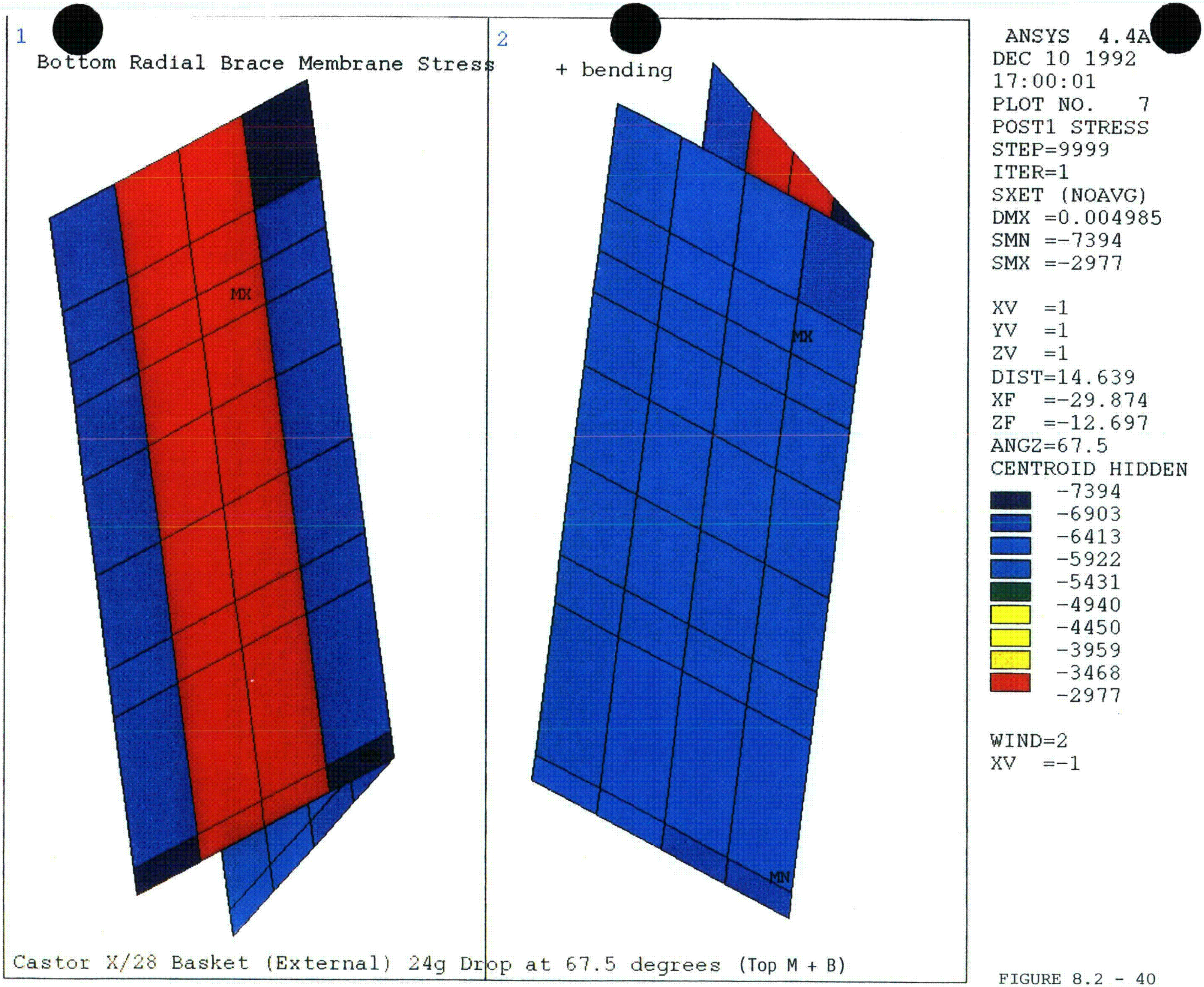
1
Bottom Radial Brace Membrane Stress
MX
2
+ bending
MX
MN
ANSYS 4.4A
DEC 10 1992
17:00:01
PLOT NO. 7
POST1 STRESS
STEP=9999
ITER=1
SXET (NOAVG)
DMX =0.004985
SMN =-7394
SMX =-2977
XV =1
YV =1
ZV =1
DIST=14.639
XF =-29.874
ZF =-12.697
ANGZ=67.5
CENTROID HIDDEN
-7394
-6903
-6413
-5922
-5431
-4940
-4450
-3959
-3468
-2977
WIND=2
XV =-1
Castor X/28 Basket (External) 24g Drop at 67.5 degrees (Top M + B)

FIGURE 8.2 - 40

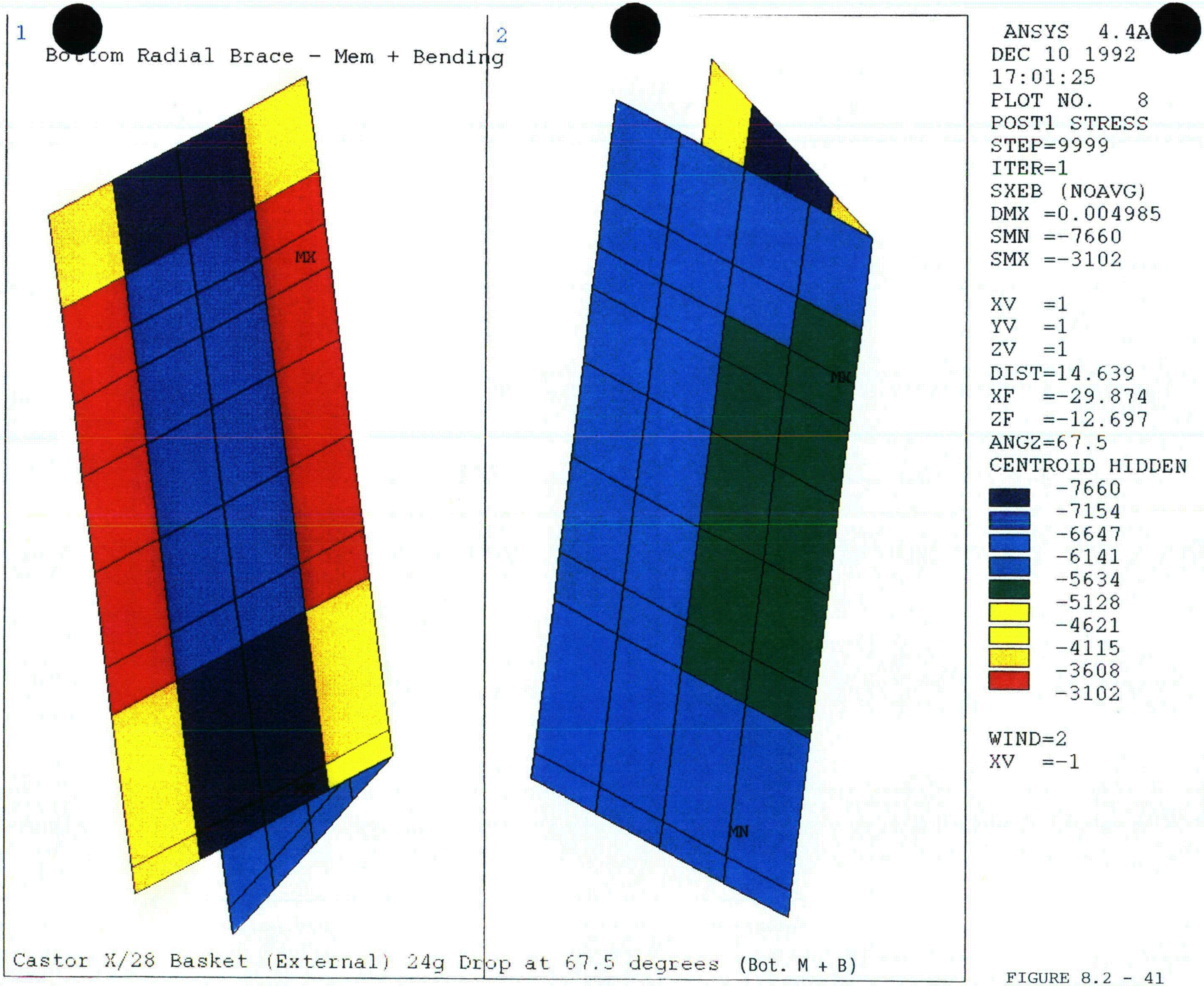
1
Bottom Radial Brace - Mem + Bending
MX
2
MX
MN
Castor X/28 Basket (External) 24g Drop at 67.5 degrees (Bot. M + B)
ANSYS 4.4A
DEC 10 1992
17:01:25
PLOT NO. 8
POST1 STRESS
STEP=9999
ITER=1
SXEB (NOAVG)
DMX =0.004985
SMN =-7660
SMX =-3102
XV =1
YV =1
ZV =1
DIST=14.639
XF =-29.874
ZF =-12.697
ANGZ=67.5
CENTROID HIDDEN
-7660
-7154
-6647
-6141
-5634
-5128
-4621
-4115
-3608
-3102
WIND=2
XV =-1

FIGURE 8.2 - 41

Table 8.2-4
Summary of Maximum Stresses in the CASTOR X/28 Basket
Due to Accidental Tip-over in Various Orientations of the Basket

Component	Maximum Stress (psi)	Allowable Stress (psi)	Factor of Safety
Inner Basket 0° Orientation	12,838	30,240	2.4
	21,834	45,360	2.1
Outer Basket 0° Orientation	-5,945	33,170	5.6
	44,127	49,750	1.1
Inner Basket 45° Orientation	10,305	30,240	2.9
	24,594	45,360	1.8
Outer Basket 45° Orientation	-5,560	33,170	6.0
	33,521	49,750	1.5
Inner Basket 67½° Orientation	4,562	30,240	6.6
	21,863	45,360	2.1
Outer Basket 67½° Orientation	11,929	33,170	2.8
	19,006	49,750	2.6

NOTES:

(1) Inner basket allowable stresses based on 350°C temperature.

(2) Outer basket allowable stresses based on 260°C temperature.

(3) Factor of Safety = Allowable Stess / Calculated Stress

Buckling Evaluation of the Fuel Separating Plates

Due to the tip-over accident of the cask, the fuel separating plates experience a combined compressive and bending stresses. The effect of these stresses on the stability of the fuel basket is evaluated in this section. The separating plates of the basket can be considered to be plate (or shell) type component support, as classified by the ASME code Section III Subsection NF. For this type of the component support, Appendix F of the ASME code does not put a requirement for combining axial compression and bending stresses. To be conservative, however, the axial compression and bending stresses are combined per the guidelines of the Non-Mandatory APPENDIX A, Section A-9000.

The interaction equation to be used for the simple or complex bending and compression, per Table A-9210(d)-1 is:

$$\frac{f_c}{F_c} + \frac{f_b}{F_b} < 1.0$$

where,

f_c = Applied compressive stress, psi
F_c = Allowable compressive stress, psi
f_b = Applied bending stress, psi
F_b = Allowable bending stress, psi

The code also requires that the amplification of bending moment by axial load be taken into account. This can be accomplished by multiplying the bending stress by an amplification factor k (see Design of Welded Structures by Omer W. Blodgett, Page 2.11-7 /Ref. 8.2-23/), such that:

$$k = \frac{1}{1 - \frac{f_c}{F_e'}}$$

where,

$$F_e' = \frac{\pi^2 E}{1.3\ K\ (l/r)^2} \qquad \text{Appendix F-1334.5(b)}$$

E = Modulus of elasticity of the material, psi
K = Effective length factor
l = Actual unbraced length in plane of bending, in
r = Radius of gyration about axis of current bending, in

The interaction equation thus becomes:

$$\frac{f_c}{F_c} + \frac{f_b}{(1 - f_c/F_e')F_b} < 1.0 \qquad \text{..........................(1)}$$

Please note that this equation is similar to equation (20) of NF-3321.1(e) for the linear type component support.

Allowable Bending Stress

The allowable bending stresses for use in the interaction equations is limited to the greater of $1.2S_y$ and $1.5S_m$ but not larger than $0.7S_u$ (F-1334.7). At the highest basket temperature of 350°C, from Table 3.2-4(b)

$$S_y = 18{,}900 \text{ psi}$$
$$S_m = 12{,}600 \text{ psi}$$
$$S_u = 46{,}000 \text{ psi}$$

Therefore,

$$F_b = \text{greater of (22,680 and 18,900) but} < 32{,}200$$
$$= 22{,}680 \text{ psi}$$

Allowable Compressive Stress

The allowable compressive stress to be used in the interaction equation is taken to be 2/3rd of the buckling stress of the plate under consideration (F-1334.3(a)). The buckling stress of the plates are dependent on the thickness and the unsupported length. The CASTOR X/28 basket consists of two different sizes of separating plates. As shown in Figure 8.2-42, the inner basket separating plates are 20mm thick and 569mm wide. The outer basket separating plates which form a delta shape are 10mm thick and 228mm wide. All the plates extend to the entire length of the basket and are 4110mm long.

The buckling stress of a particular size plate can be calculated by idealizing the boundary conditions and the loading as shown in Figure 8.2-43. For these conditions the buckling stress can be obtained from any standard reference book (e.g. Roark & Young). For a/b < 0.2, the critical buckling stress is same as the one obtained from considering a unit width of the plate as a column and using the Euler buckling formula for the buckling stress. Thus,

$$\sigma_{cr} = \frac{\pi^2 E}{12} (t/l)^2$$
$$= 0.8225 \text{ E } (t/l)^2$$

$$f_c = 2/3\ \sigma_{cr}$$
$$= 0.5483 \text{ E } (t/l)^2$$

$$E = 25.45 \times 10^6 \text{ psi at 350°F}$$ (see Table 3.2-3(d))

The 20mm thick plates are 569 mm long and have various intermediate supports. Conservatively neglecting the beneficial effects of reduction in the effective length factor K due to these supports, i.e assuming K = 1.0, the allowable compressive stress is:

$$F_c = 0.5483 \times 25.45 \times 10^6 \times (20/569)^2$$
$$= 17{,}240 \text{ psi}$$

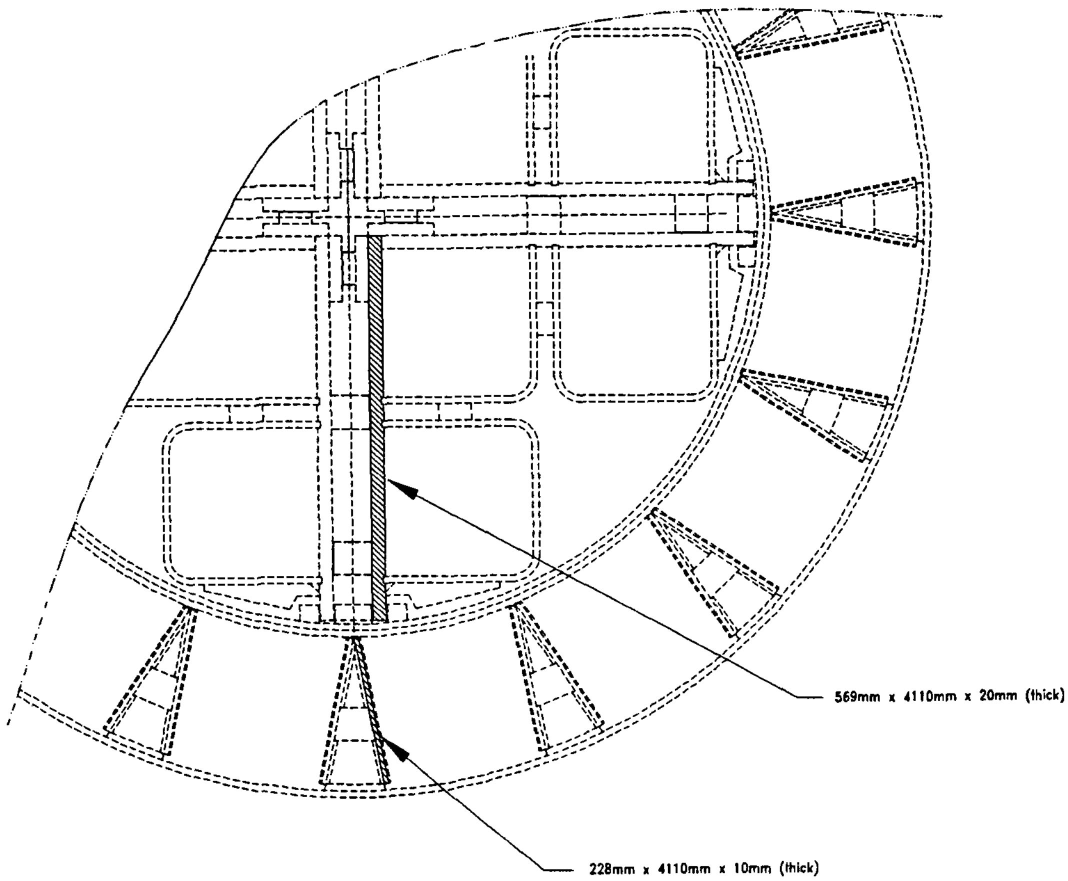

Figure 8.2-42
CASTOR X/28 Basket Fuel-Separating Plates

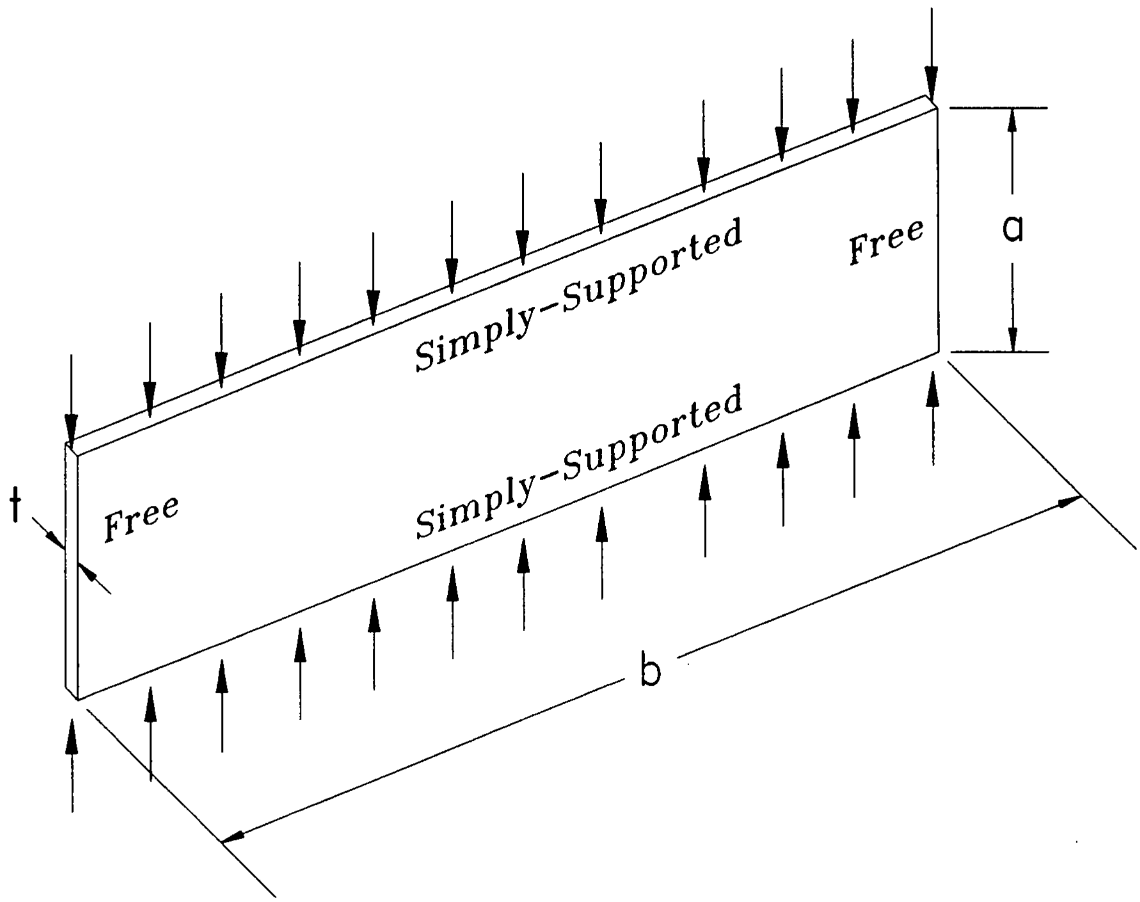

Figure 8.2-43
Fuel-Separating Plate Idealization

and,

$$F_e' = \frac{\pi^2 E}{1.3\ K\ (l/r)^2}$$

$$= \frac{\pi^2 E}{12x1.3x1.0}\ (t/l)^2$$

$$= 0.6327\ E\ (t/l)^2$$

$$= 0.6327 \times 25.45 \times 10^6 \times (20/569)^2$$

$$= 19{,}912 \text{ psi}$$

The 10mm plates are 228mm long and have a Radionox cladding attached to them. Conservatively, neglecting the beneficial effects of this cladding, the allowable compressive load for these plates are:

$$F_c = 0.5483 \times 25.45 \times 10^6 \times (10/228)^2$$

$$= 26{,}843 \text{ psi}$$

and,

$$F_e' = 0.6327 \times 25.45 \times 10^6 \times (10/228)^2$$

$$= 30{,}975 \text{ psi}$$

Applied Stresses

The stresses obtained from the finite element analysis of the basket due to tip-over in various orientations (0°, 45° and 67½°), are separated out into the uniform compressive stresses and the maximum bending stresses. The stresses were obtained from stress contour plots of the finite element model as follows.

The stress contour plots used to obtain the stress components used in the buckling interaction equations are shown in Figures 8.2-18 through 8.2-41. The stresses are tabulated in Table 1. These plots were obtained from the ANSYS Postprocessor, POST1. The element stress was stored as a stress item using the notation

SXEM = Membrane Stress, X-direction
SXET = Top Surface Stress (M + B) X-direction
SXEB = Bottom Surface Stress (M + B) X-direction

and additional components SYEM, SYET, SYEB having the same meaning except for the Y direction. Note that the plots show the stress label on the eighth item down on the top right-hand side of each plot. The nomenclature, M + B indicates membrane plus bending, Top refers to the top surface of the element, and Bottom (or Bot) refers to the bottom or opposite surface of the shell element. It is noted that the "top" and "bottom" surfaces are arbitrary and depend only upon the order in which the nodes which define each element are specified, i.e., clockwise or counterclockwise. The ANSYS shell element, STIF63, which was used in this analysis, calculates membrane stress at the middle surface and membrane plus or minus bending stress at the top and bottom surfaces. Centroidal stresses were used in this evaluation, thus the stress plots indicate a constant stress over each element with no stress averaging at element edges (or nodes). This is the reason that the plots indicate (NOAVG)

in the eighth line down and each element is shown as a single color rather than a continuously varying gradient over the surfaces.

The buckling evaluation procedure was as follows: the analyses were divided into six cases. These include (1) the internal structure and (2) external structure for three orientations, 0°, 45°, and 67½° impact angles. For each case, the stress items were selected and plotted. The X-direction of the element is defined by the order of the node definitation where the element X becomes the first two nodes defined, i.e., from node i toward node j. It was determined that the X-direction was the basket "radial" direction and y was along the axis of revolution of the Cask, thus, X-direction stresses were used in the evaluation. The y stresses were also reviewed and were very small in all cases as would be expected.

The membrane X stresses were then plotted for each case. For example, Figure 8.2-18 shows the membrane stresses for Case 1, the 0° orientation for the inner structure. From this plot it can be determined that the lower 20mm plate has the highest compressive stress. Two areas are evaluated, marked A and B in Figure 8.2-18. These locations were chosen because the bending stresses are higher in these areas as can be seen from Figures 8.2-19 and 8.2-20. All elements along the length of the basket at location A were considered for the evaluation, with the highest stress at any point used in the evaluation.

The stress levels were obtained from the color map shown on the right-hand side of the plot. Since there are a very limited number of colors available, the stress range is quite high for each color. The worst case assumption was made in obtaining the stresses based upon the color of the element and the stress range indicated for each color. These values were tabulated in Table 8.2-5.

It was desired to obtain the worst case combination of membrane and bending according to equation (1). Thus, the tabulated stresses were used to separate the compressive membrane component from the membrane plus bending component which is plotted at the top and bottom surfaces of the element. Case 1 of Table 8.2-5, for example, shows a membrane stress of -3,635 psi and M + B stresses of -12,118 psi and 10,447 psi at the top and bottom surfaces, respectively. If we combine -3,635 with -12,118 we would calculate a bending stress of (12,118 - 3,635) or +8,483 psi. Combining -3,635 with the tensile stress 10,447 results in a bending stress of 14,082 psi which was used in the evaluation of equation (1). This is a very conservative method for the following reasons: (A) the highest values of the stress range in the color plot legend were used to evaluate each component, and (B) it was assumed that the highest stress components occurred at the same point, and (C) it was assumed that the state of stress at the highest point was constant along the length of the basket. This procedure may be thought of more as a screening method to find the most sensitive locations. Detailed stress printout at each element can be obtained if necessary for a more exact evaluation. This was actually done in the case of Point A, Case 1 and the exact stress values for element A are also given in Table 8.2-5. This shows that the procedure is quite conservative.

Case 2 plots are shown in Figures 8.2-21 through 8.2-24. As would be expected, the lower most separation plate exhibits the highest compressive stress. This plate was evaluated for buckling, and a rather wide margin of safety exists. Note also that the plate was assumed to

Table 8.2-5
Buckling Interaction Stresses

Case	Location	Largest Membrane f_c (psi)	Largest Membrane plus Bending, (psi)		Largest Bending f_b (psi)	Allowable Compressive F_c	Allowable Bending F_b (psi)	Factored Euler F_e' (psi)	Combined Ratio[1]
			Top	Bottom					
1 Int. Str. 0°	A	-3,635	-12,118	10,447	14,082	17,240	22,680	19,912	0.969
	A_1[2]	-1,607	-10,837	7,626	9,332	17,240	22,680	19,912	0.535
	B	-3,635	6,573	-2,059	10,198	17,240	22,680	19,912	0.761
2 Ext. Str. 0°	A	-5,033	-2,995	840	5,873	26,843	22,680	30,975	0.496
3 Int. Str. 45°	A	-2,264	6,392	6,376	8,656	17,240	22,680	19,912	0.561
4 Ext. Str. 45°	A	-4,907	-13,161	-3,751	8,254	26,843	22,680	30,975	0.614
5 Int. Str. 67½°	A	-2,631	7,758 -6,678	4,737 -9,735	10,389	17,240	22,680	19,912	0.681
6 Ext. Str. 67½°	A	-6,531	-2,977 -7,394	-3,102 -7,660	3,429	26,843	22,680	30,975	0.434

NOTES: (1) Combined Ratio is the left hand side of equation (1).

$$\frac{f_c}{F_c} + \frac{f_b}{(1 - f_c/F_e')F_b} < 1.0$$

(2) Combination at A_1 is the "exact" stress combination.

be simply supported when the interaction equation allowable stress was calculated. In fact, these plates are welded top and bottom and are more nearly "built-in" than simply supported.

Figures 8.2-25 through 8.2-27 provide stress plots for Case 3. Due to the symmetry of the geometry, the stresses are almost identical on the 20mm plates which were evaluated (marked A on the plots). The safety factor is much larger than for Case 1 as would be expected since the compressive stresses are much lower.

Case 4 results are shown on Figures 8.2-28 through 8.2-32. The highest combination of membrane compression plus bending occurs at the support points under the inner basket reaction loads. It is noted that this is the worst orientation for the external structure. This is probably due to the combined compression and bending load exerted by the inner basket on the separator plates. Also, a more exact stress distribution was obtained (Figure 8.2-32) by plotting element values rather than a color map.

Cases 5 and 6 are shown in Figures 8.2-33 through 8.2-36 and 8.2-37 through 41, respectively. The margins of safety are greater than found for Cases 1 through 4.

Based upon the analyses presented herein, it is concluded that the buckling interaction equation is satisfied by both the 10 and 20mm plates. It is shown that an adequate margin of safety exists in the design of Castor X/28 basket to preclude instability of the fuel separating plates.

DISCUSSION OF BOUNDARY CONDITIONS USED IN THE FINITE ELEMENT ANALYSIS OF THE CASTOR X/28 AND X/33 BASKETS

GNSI DOCUMENT No. ST-128

General Nuclear Systems, Inc.
Columbia, SC
December, 1992

PROPRIETARY INFORMATION

9212300285 921228
PDR PROJ
M-50 CF

DISCUSSION OF BOUNDARY CONDITIONS

CASTOR X/33 AND X/28

CASTOR X/33

Figure 1 shows the elevation view of the basket for Castor X/33. Note that circumferential bands are welded to the basket at 49" intervals. By assuming symmetry at the center of the band and the midspan between bands, the finite element model can be reduced to one-sixth of the overall length. Note that by cutting through the center of the bands, the supports at that location are cut into half the thickness that they would be at the ends. Figure 2(a) provides the shear and moment diagram as well as the reaction forces for a continuous beam simply supported at four equally spaced points with a linearly increasing load. The finite element model used in the analyses can be related to this beam by the following analogy. If we assume point A in Figure 2 is the bottom of the cask and D is the top of the cask, the relative positions along the cask shown on Figure 1 may be related to corresponding locations in Figure 2.

The basket loading is due to deceleration in the tipover accident. Noting that the cask rotates about point A, the acceleration at each point is proportional to the distance from point A; i.e., $a = R\alpha$. Where: a = acceleration at any point, R = the distance from A to a point along the cask and α is the angular or rotational acceleration. The assumed boundary conditions for the analysis are identical to those for a uniformly loaded beam where w = the load per unit length. If we take w to also be the value of the maximum linear loading shown in Figure 2(a), then Figure 2(b) represents the loading on the cask if the portion from point (c) to the midspan is modeled. Comparing Figures 2(a) and 2(b), it can be seen that the values of both shear and moment loading at point C are larger in the beam shown on 2(b), which is analogous to the finite element model, than at point C in 2(a), which is analogous to the actual loading.

Thus by modeling the section at the circumferential band C, the largest shear and moment loads were evaluated. Further, the finite element model utilizes planer symmetry and, as previously stated, the band width modeled in the finite element representation was only 100 mm and all gusset plates were modeled at half of their actual thickness. Additionally, the large diameter of the basket as compared to its length insures that the moment effect is small compared to the shear effect. Little or no rotation of the basket cross section due to bending will be experienced with the majority of the deformation being caused by the shear load.

The boundary conditions applied to the X/33 basket included the following, (1) axial displacement of zero at the circumferential band location for all nodes in the plane of the band (including all separator plates and sleeves). (2) Nodal coupling of axial degrees of freedom at the midspan for all separator plates and for each sleeve, i.e., the sleeve coupled nodes are only those nodes on a particular sleeve. The main separator plate nodes are all coupled together since these plates are welded together. Nodal coupling of degrees of freedom are specified in ANSYS by indicating that all degrees of freedom identified in a given set have the same deflection but not necessarily a zero deflection. Nodal Couplings were used since the basket should be free

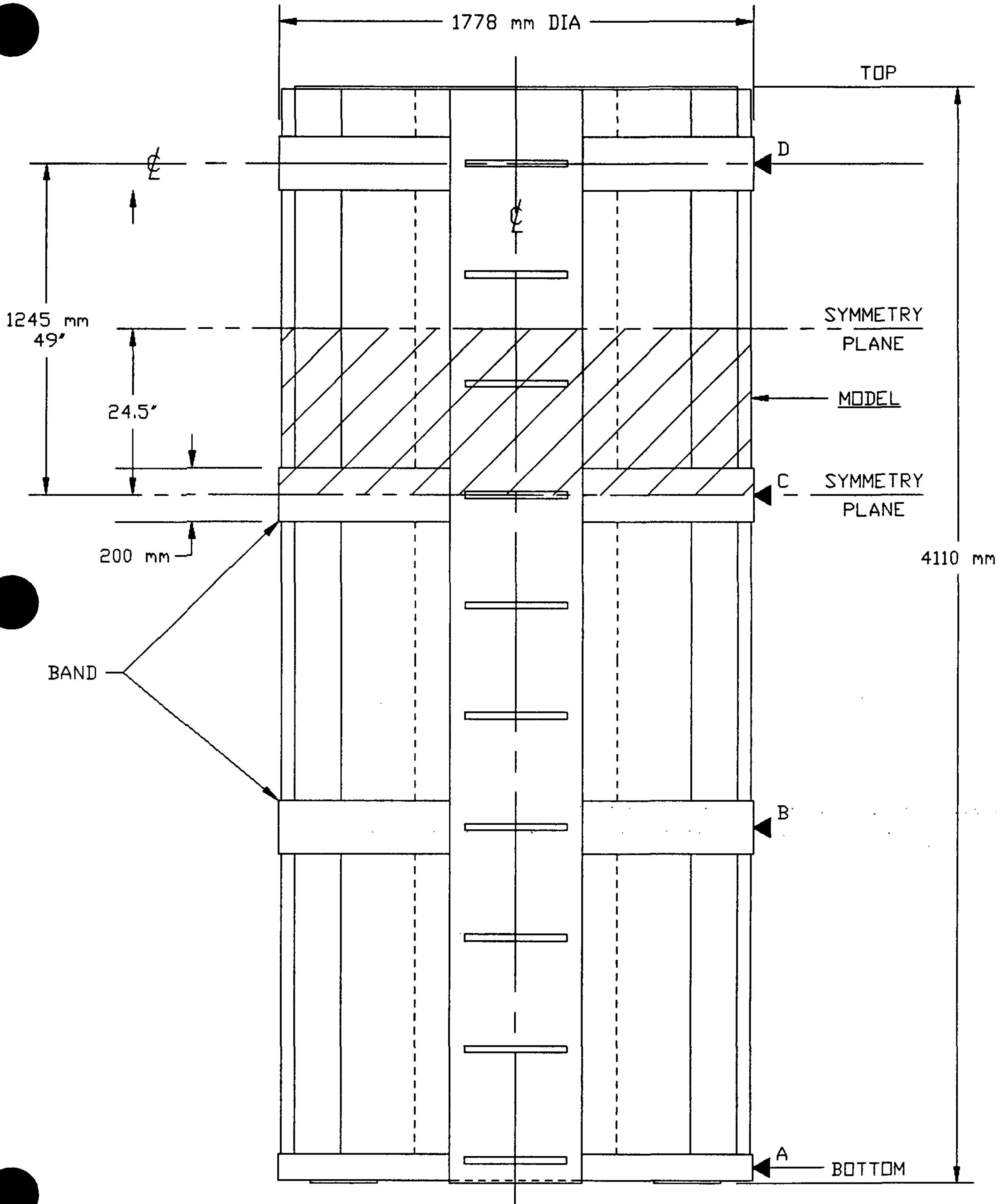

FIGURE 1 - Castor X/33 Basket - Elevation View

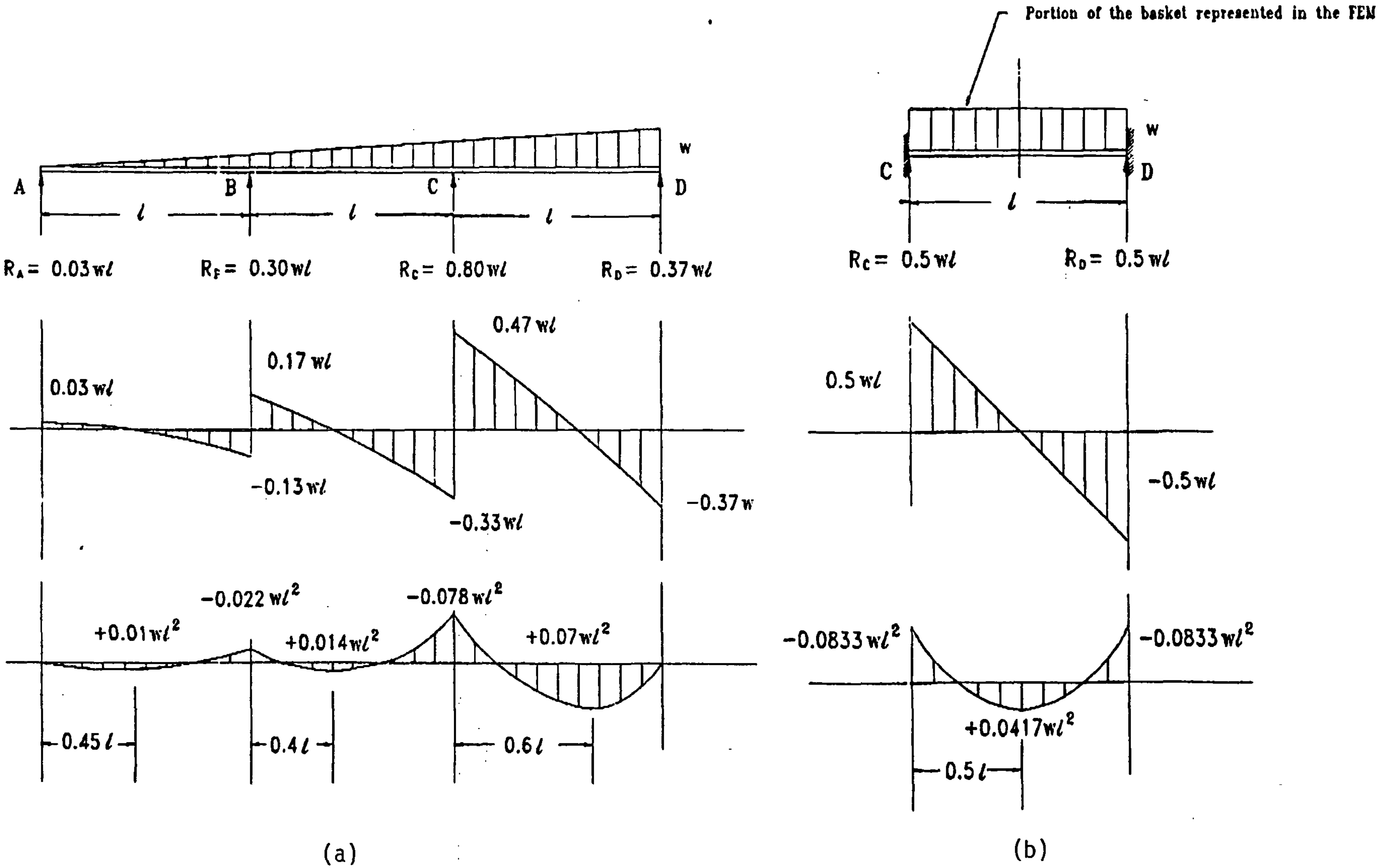

FIGURE 2 - Beam Analogy for Castor Boundary Conditions

to expand in the axial direction. This condition is similar to generalized plane strain in a two-dimensional problem where the component is free to expand axially but the axial strain component must be constant at all planer cuts. (3) Radial displacements of zero at the circumferential bands for all nodes that want to grow radially outward. For nodes which tend to move inwardly, i.e., separate for the wall of the cask, the nodes were free to move radially. No other nodal points were fixed except in the 360° model where one point is used to prevent tangential motion axis, i.e., stabilize the problem. For the 180° half model used for the tipover analyses, symmetry boundary conditions were used to represent the opposite half model. This includes zero lateral displacement at the centerline for solid elements and zero rotation angle for out of plane rotation for the shell elements (i.e., enforcement of zero slope across the symmetry plane).

A combination of shell and solid elements were used in the model. This was done to better represent the actual geometry. For the thinner plates which would be difficult to represent with solid elements and retain an acceptable aspect ratio, shell elements were used. For the thicker plates, solid elements were used. The use of solid elements allows for better characterization of the geometry since the actual plate dimensions are represented by the nodal pattern. Shell elements necessitate the use of centerline geometries, thus, it is impossible to correctly model the true geometry. It has been shown that the ANSYS STIF45 solid element is capable of accurately predicting linear bending with one element through the thickness. This element utilizes a quadratic shape function which allows for a linear strain distribution within the element. Thus, bending stresses as well as membrane stresses can be predicted with excellent results. The ANSYS Verification Manual contains examples which illustrate this accuracy. Verification problem 17 is attached.

CASTOR X/28 BOUNDARY CONDITIONS

The X/28 basket was evaluated using two separate models. This was done because at the time these models were developed the model size was somewhat limited by storage capability of available computers. The use of separate models allowed for a more accurate analysis since more elements could be used in each part of the model.

The design of the X/28 basket is such that the models may easily be separated without loss of generality or accuracy. The outer ring of 16 elements fits into the cask as a single unit. The analysis clearly shows that this ring is very rigid and the deflection of the outer basket is quite small, thus, the clearance between the inner and outer basket will not be taken up by deformation during the accident.

The inner basket is actually four separate segments with a capacity of three fuel elements each. The baskets are shown in Figures 3 and 4 for two drop orientations.

For the 90-270° drop (Figure 3), the boundary condition plots for the outer basket are shown on Figures 5 and 6. The lower 180° of the basket are fixed in the radial direction. Symmetry conditions are applied at the vertical centerline. Axial motion was prevented at Z = 0 and nodal couplings were applied at the opposite end of the model. Figure 5 shows these conditions on a nodal plot, and Figure 6 shows the same boundary conditions superimposed on

VERIFICATION PROBLEM NO. 17

TITLE: Bending of a Solid Beam.

TYPE: Static analysis (KAN=0), solid elements (STIF45).

REFERENCE: Roark (Ref. 6), Pages 104, 106.

PROBLEM: A beam of length L and height h is built-in at one end and loaded at the free end with 1) a moment M, and 2) a shear force F. For each case, determine the deflection δ at the free end and the bending stress σ_{Bend} 1 in. from the wall at the outside fiber. See Verification Problem No. 16 for loading sketches and given input quantities.

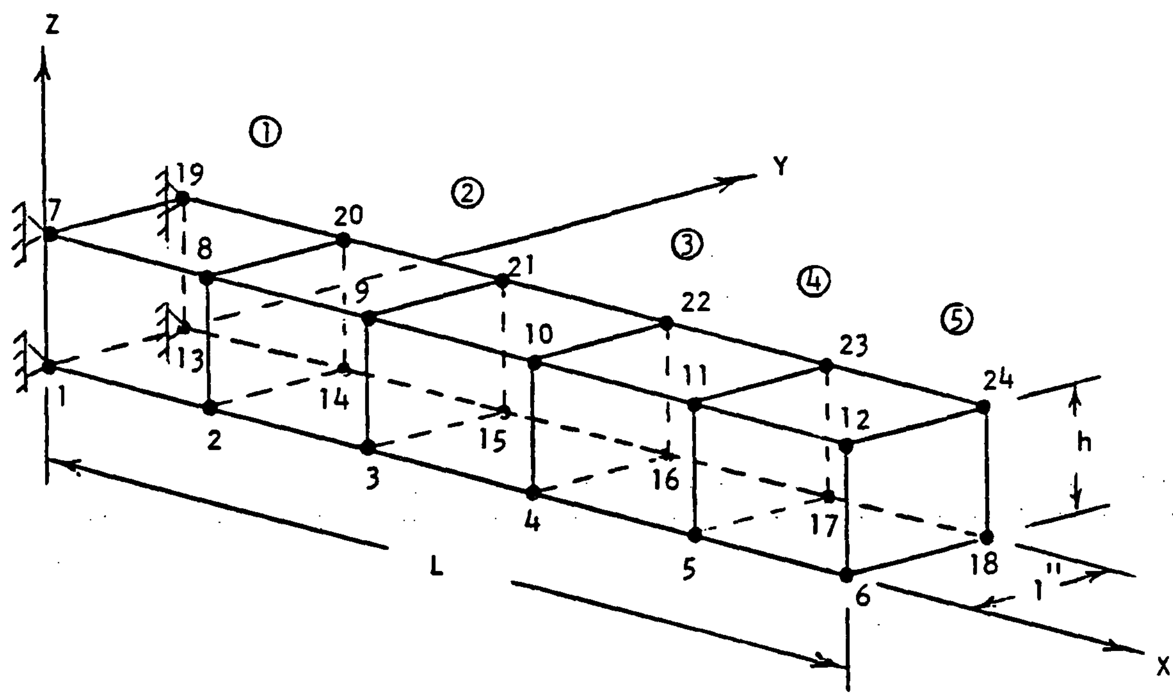

Finite Element Model.

MODELING HINTS: The stiffness matrix formed in the first load step is also used in the second load step. The end moment is represented by discrete nodal force couples.

VERIFICATION PROBLEM NO. 17 (Continued)

INPUT DATA LISTING:

```
/PREP7
/TITLE, VM17, BENDING OF A SOLID BEAM (SOLID ELEMENTS)
C***          FORMULAS FOR STRESS AND STRAIN, ROARK, 4TH ED.
C***          USING STIF45 ELEMENTS
ET,1,45,,,,,,2
EX,1,30E6
NUXY
N,1
N,6,10
FILL
N,7,,,2
N,12,10,,2
FILL
NGEN,2,12,1,12,1,,1
E,7,8,2,1,19,20,14,13
EGEN,5,1,1
ITER,1,1
/TITLE, VM17, CASE 1 - END MOMENT, ROARK, PAGE 106, NO. 9
D,1,ALL,,,19,6
F,6,FX,500,,18,12
F,12,FX,-500,,24,12
LWRITE
/TITLE, VM17, CASE 2 - END LOAD, ROARK, PAGE 104, NO. 1
F,6,FX,,,24,6
F,6,FZ,75,,24,6
LWRITE
/TITLE, VM17, BENDING OF A SOLID BEAM (SOLID ELEMENTS)
AFWRITE
FINISH
/INPUT,27
FINISH
```

SOLUTION COMPARISON:

	Case 1		Case 2	
	δ, in	σ_{Bend}, psi	δ, in	σ_{Bend}, psi
Theory	0.00500	3000.	0.00500	4050.
ANSYS	0.00500	3000.	0.00505	4050.
Difference	None	None	1.0%	None

VERIFICATION PROBLEM NO. 16

TITLE: Bending of a Solid Beam.

TYPE: Static analysis (KAN=0), plane stress elements (STIF42).

REFERENCE: Roark (Ref. 6), Pages 104, 106.

PROBLEM: A beam of length L and height h is built-in at one end and loaded at the free end with 1) a moment M, and 2) a shear force F. For each case, determine the deflection δ at the free end and the bending stress σ_{Bend} 1 in. from the wall at the outside fiber.

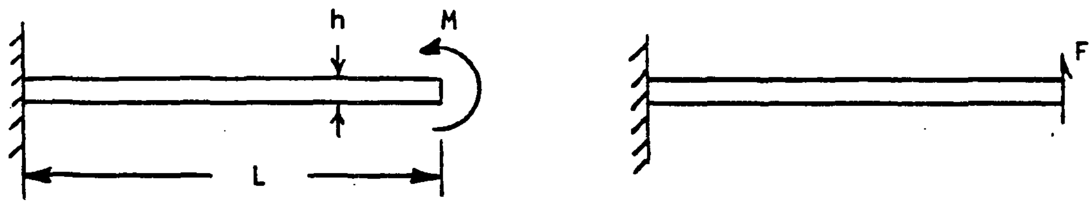

Case 1 Case 2

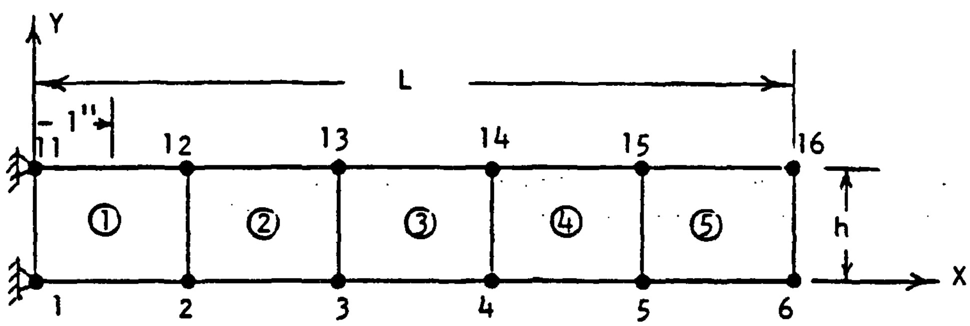

Finite Element Model

GIVEN: L = 10 in, h = 2 in, M = 2,000 in-lb, F = 300 lb, E = 30E6 psi, ν = 0.0

MODELING HINTS: The stiffness matrix formed in the first load step is also used in the second load step. The end moment is represented by equal and opposite forces separated by a distance h. The bending stress is obtained from face stresses on element 1.

D = RADIAL DISPLACEMENT = 0
T = TANGENTIAL DISPLACEMENT = 0
G = GAP - OPEN IF TENSION
- CLOSED IF COMPRESSION
F = REACTION FORCE FROM INNER BASKET
F_T = TANGENTIAL FORCE
F_T = RADIAL FORCE

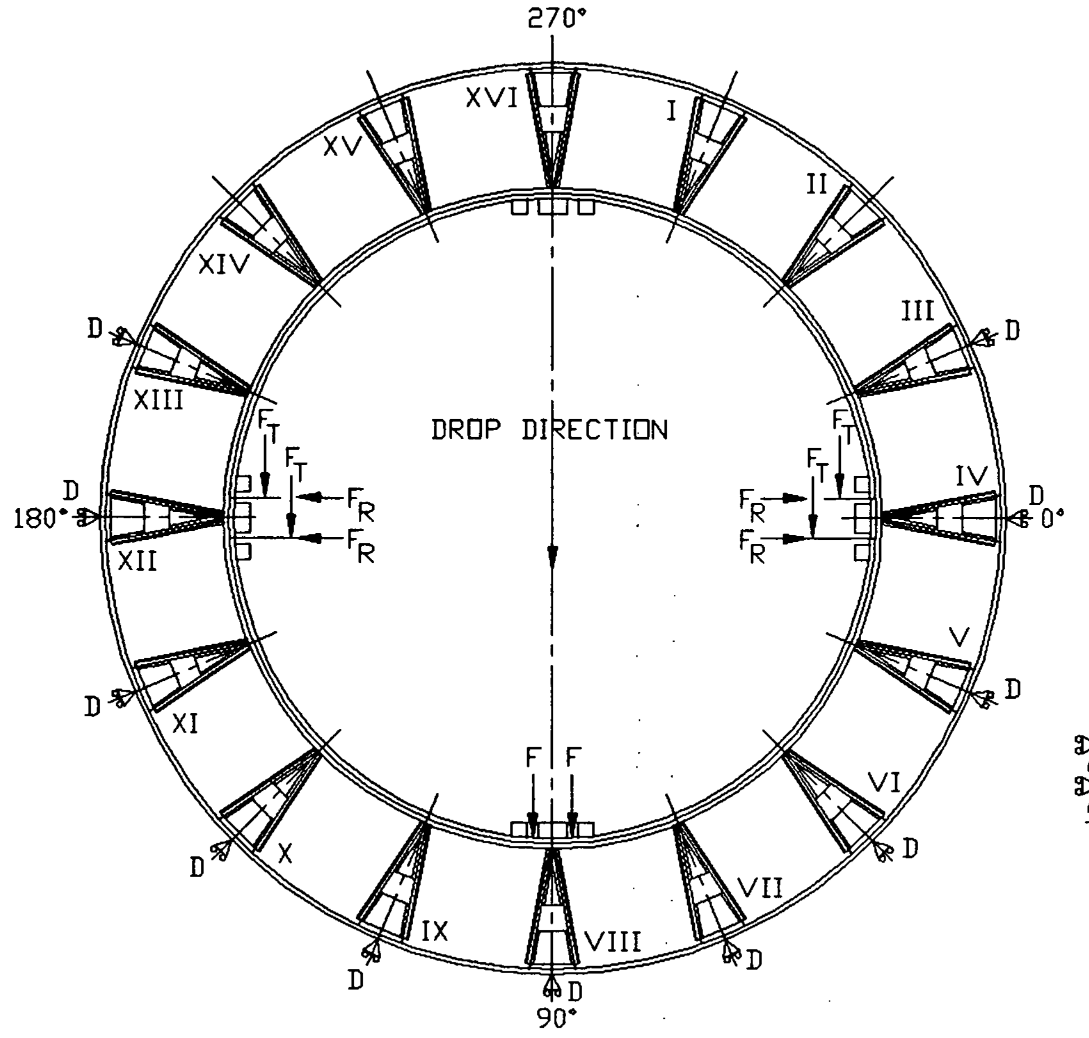

OUTER BASKET

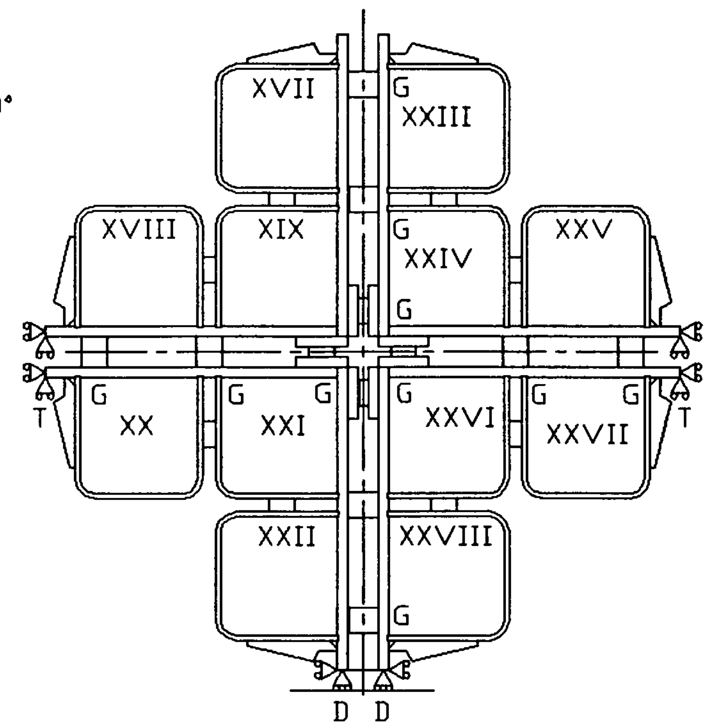

INNER BASKET

FIGURE 3 - X/28 basket vertical orientation

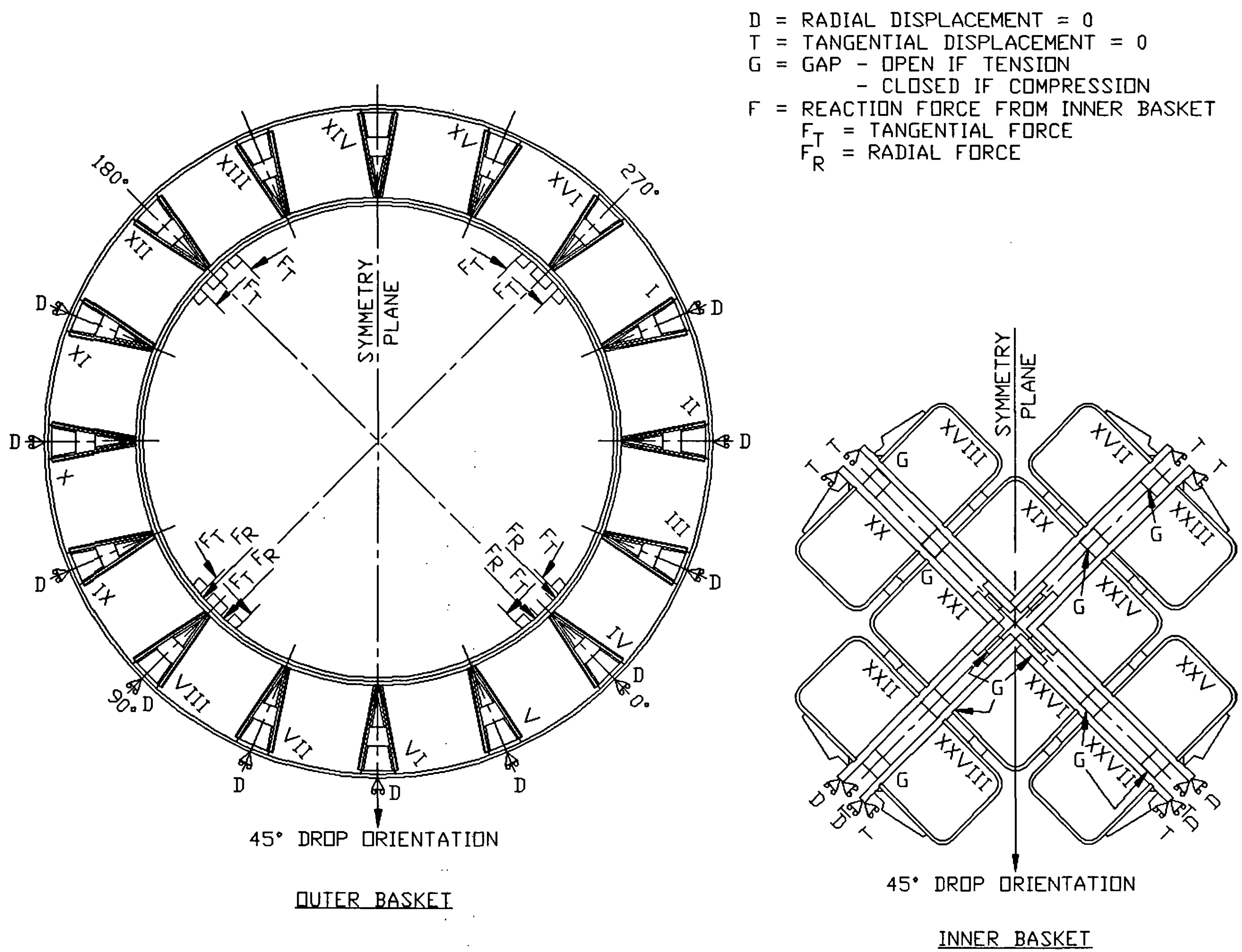

FIGURE 4 - X/28 Basket - 45 degree drop orientation

9 of 16

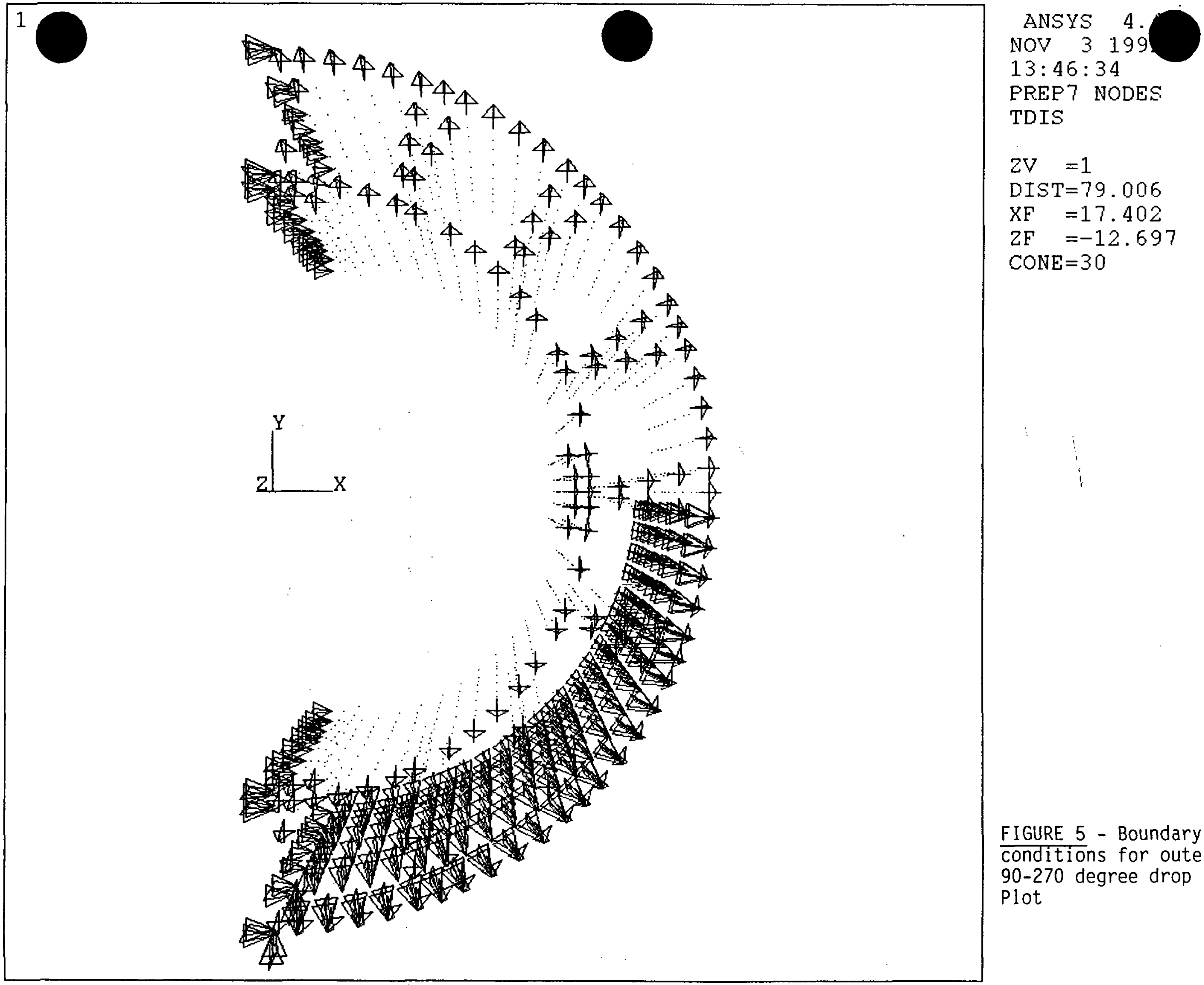

FIGURE 5 - Boundary conditions for outer basket, 90-270 degree drop - Node Plot

Castor X/28 Basket - Exterior

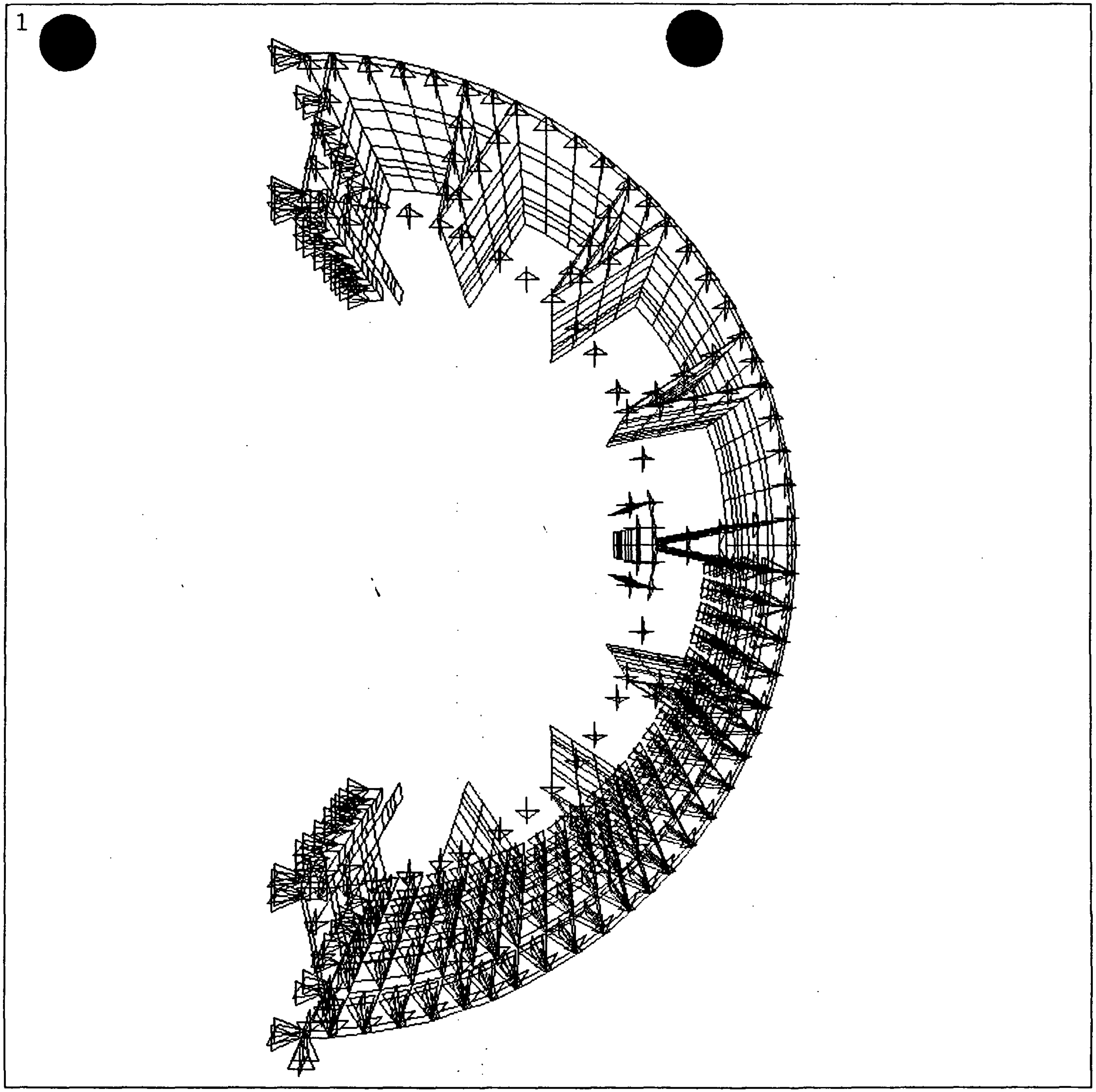

FIGURE 6 - Boundary conditions for outer basket, 90-270 degree drop - Element Plot

Castor X/28 Basket - Exterior

an element plot of the same model.

The arrows in the plots indicate the direction of restraint. Note that the arrowhead is actually represented by two triangles at right angles. This is to allow for three-dimensional viewing and should not be mistaken for a moment restraint. When viewed directly head-on, the arrowhead appears to be a + sign. The plots shown have a prospective or vanishing point angle such that the near end appears to be larger than the trailing end. For example, the nodes in Figure 5 can be seen to converge toward a point near the central triad. Note that all the nodes on the outside surface of the outer basket are rotated into a R-θ coordinate system so that the radial displacement may be restrained while not inhibiting tangential motion.

Figure 6 indicates these same boundary conditions superimposed upon the elements of the model. Both plots are included to facilitate easier interpretation. The inner basket boundary condition for the 90-270° drop orientation are shown in Figures 7 and 8. These boundary conditions represent the schematic of Figure 3, but only 180° of the basket is modeled. Symmetry conditions allow for eliminating the left-hand side.

The inner basket was run first and the reaction forces were found from this analysis. These forces were applied to the outer model as indicated in Figures 3 and 4.

Figures 9 and 10 show boundary conditions for the 45° drop orientation on the node and element models, respectively. Note that a full 360° model was utilized and the lower parts of the basket were supported both radially and tangentially, but only tangential support was applied to the upper basket supports. Thus, only compressive forces were allowed as would be the actual case.

In all cases for the inner basket, the four sections are free to move relative to each other. Thus, small clearances between the inner baskets and outer baskets can be accommodated by a slight relative motion between the components. The spacers between the baskets are only attached to one quarter segment and, thus, they will hold the baskets apart but are able to slide to accommodate clearance between this inner and outer basket.

It should also be noted that the radial gap between the inner basket and the outer basket is 4mm, whereas the tangential gap is 2mm. The radial gap is included for two purposes. The first is to allow for initial assembly of the basket. The second reason is to allow for differential expansion of the inner basket relative to the outer basket. It may be seen from the fuel rod temperature calculations that the average temperature of the inner basket is approximately 120 to 150°C higher than the outer basket temperature. The inner basket will thus expand radially outward closing the gap during operation.

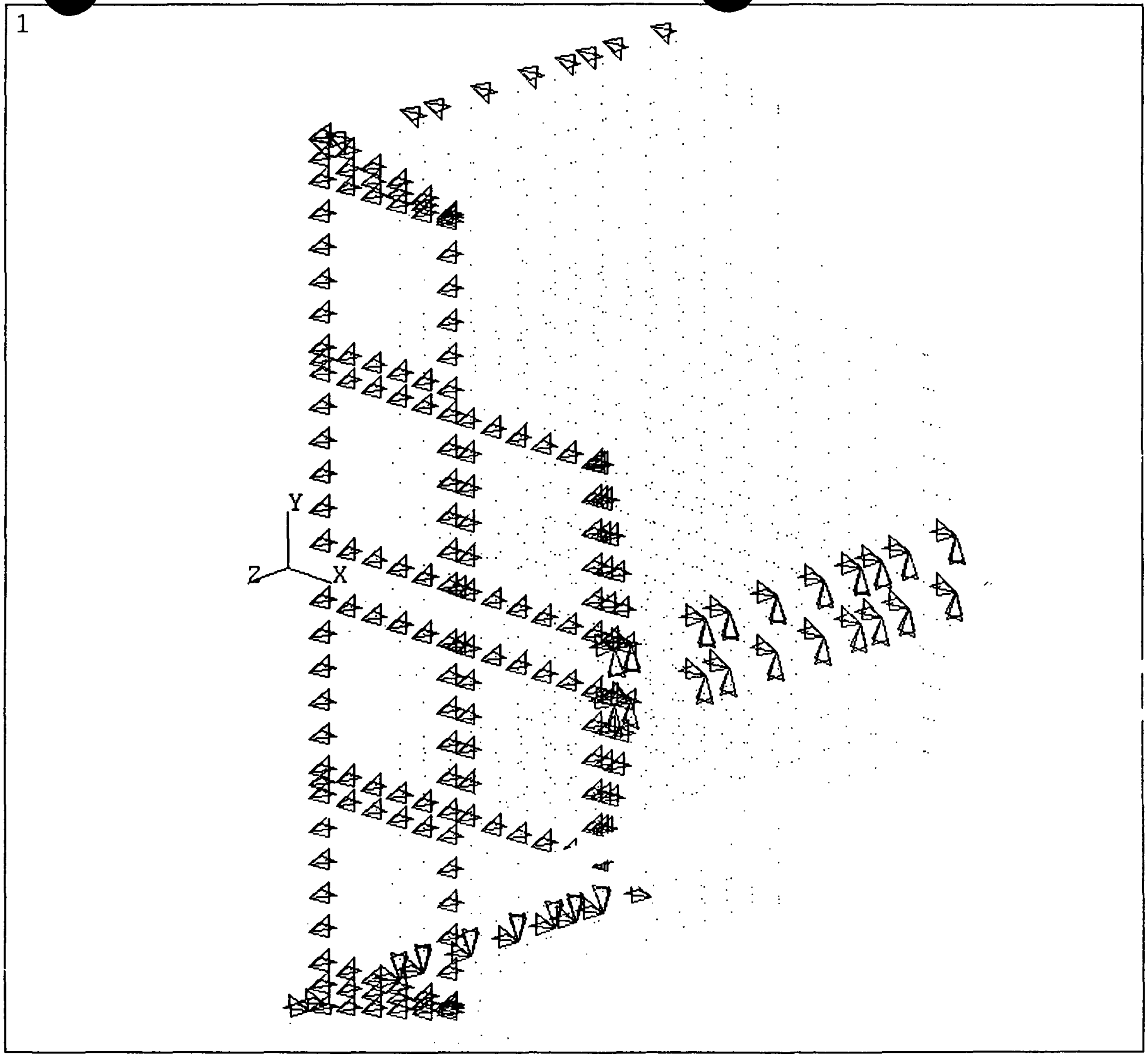

FIGURE 7 - Boundary conditions on the inner fuel basket - 90-270 degree drop - Node Plot

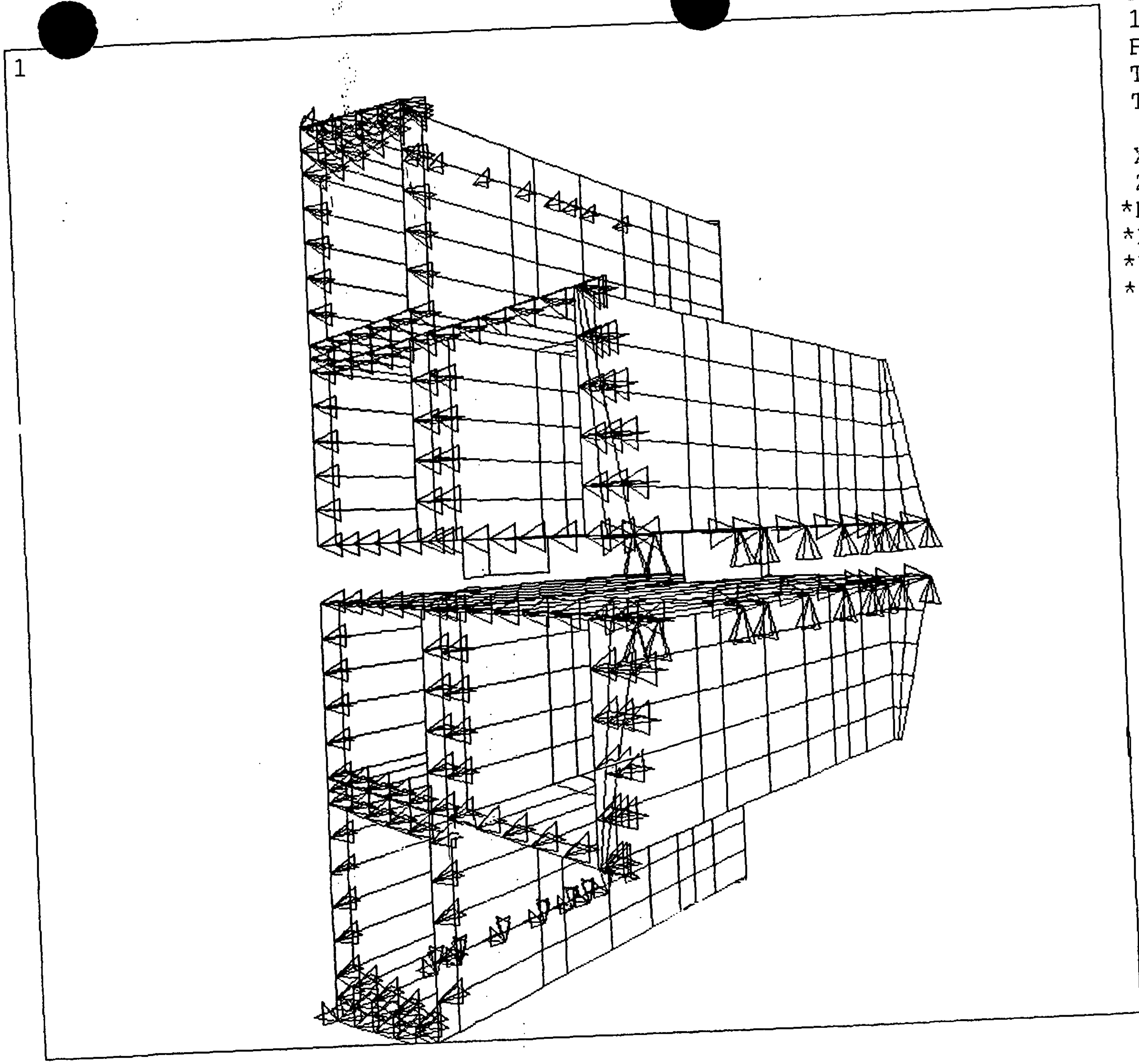

FIGURE 8 - Boundary conditions on the inner fuel basket - 90-270 degree drop · Element Plot

Castor X/28 - Internal structures

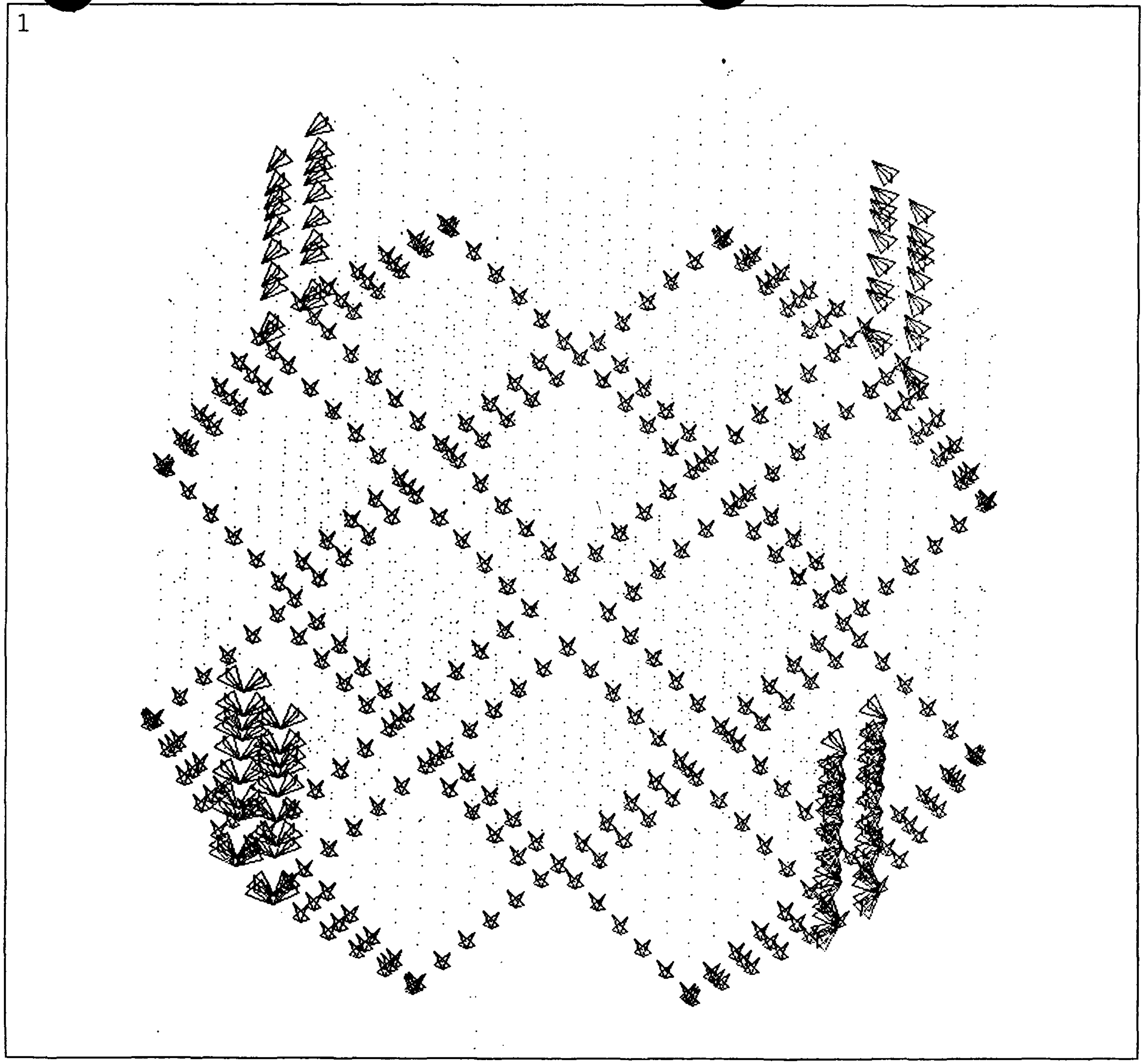

ANSYS 4.
NOV 3 199
13:51:12
PREP7 NODES
TDIS

XV =0.3
YV =0.3
ZV =1
*DIST=30
ZF =-12.697
ANGZ=45
PRECISE HIDDEN

FIGURE 9 - Boundary conditions on the inner basket - 45 degree drop - Node Plot

Castor X/28 Inner basket at 45 degrees

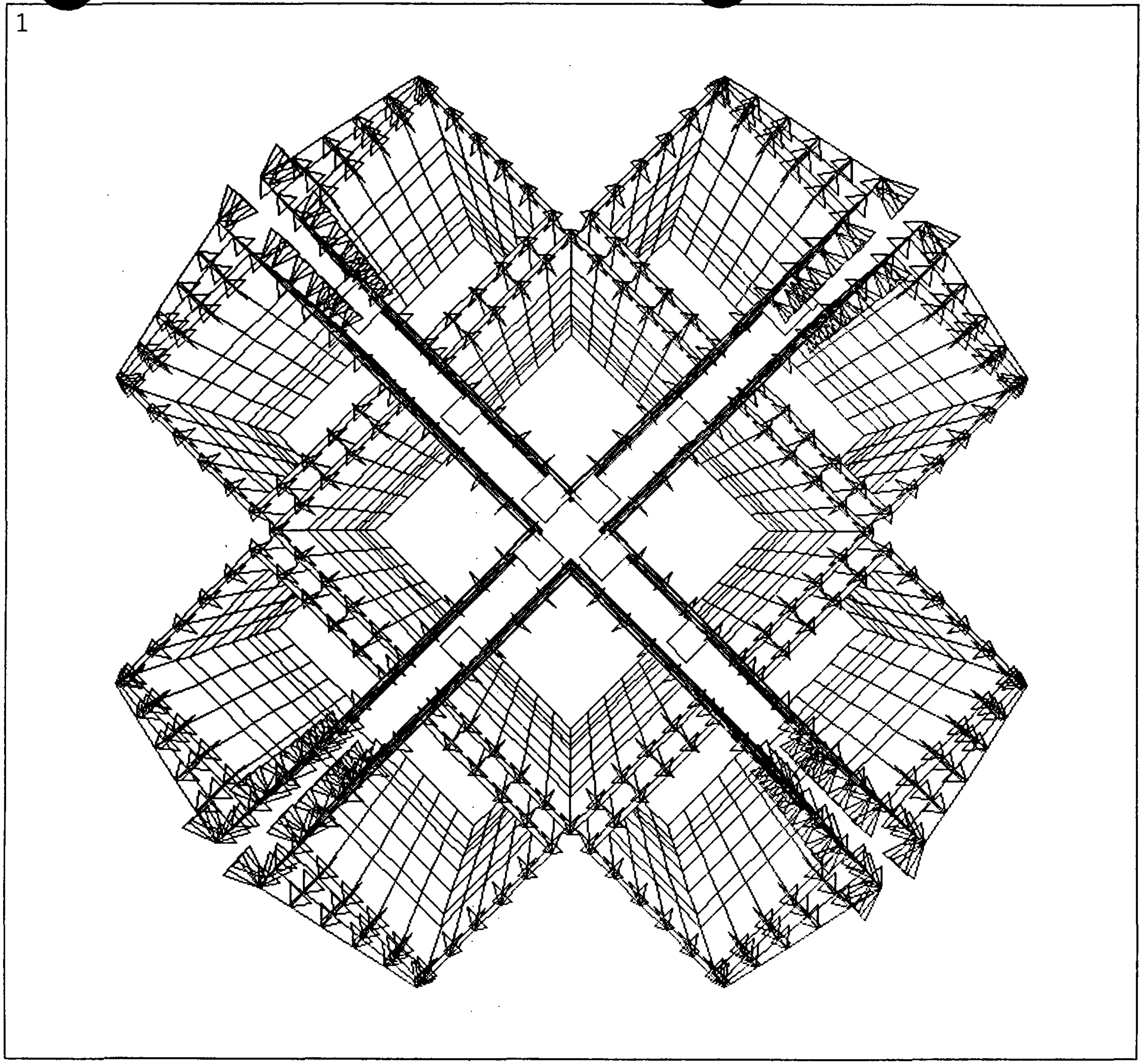

ANSYS 4.
NOV 3 199
13:52:08
PREP7 ELEMENTS
TYPE NUM
TDIS

ZV =1
*DIST=60
ZF =-12.697
ANGZ=45
CONE=30
PRECISE HIDDEN

FIGURE 10 - Boundary conditions in the inner basket - 45 degree drop - Element Plot

Castor X/28 Inner basket at 45 degrees